HHS Public Access

Author manuscript

J Med Chem. Author manuscript; available in PMC 2016 March 12.

Published in final edited form as:

J Med Chem. 2015 March 12; 58(5): 2406–2416. doi:10.1021/jm5019115.

Design, Synthesis and Biological Evaluation of Theranostic Vitamin-Linker-Taxoid Conjugates

Jacob G. Vineberg[†], **Tao Wang**[†], **Edison S. Zuniga**[†], and **Iwao Ojima**[†,‡,*]

[†]Department of Chemistry, Stony Brook University, Stony Brook, NY 11794-3400

[‡]Institute of Chemical Biology & Drug Discovery, Stony Brook University, Stony Brook, NY 11794-3400

Abstract

Novel tumor-targeting theranostic conjugates **1** and **2**, bearing either a fluorine-labeled prosthetic as a potential ^{18}F-PET radiotracer (**1**) or a fluorescence-probe (**2**) for internalization studies *in vitro*, were designed and synthesized. We confirmed efficient internalization of **2** in biotin-receptor positive (BR+) cancer cells via receptor-mediated endocytosis (RME) based on flow cytometry and confocal fluorescence microscopy (CFM) analyses, which exhibited very high specificity to BR+ cancer cells. The potency and cancer-cell selectivity of **1** were evaluated against MX-1, L1210FR and ID8 cancer cells (BR+), as well as L1210 cells and WI38 normal human lung fibroblast cells (biotin-receptor negative: BR−). In particular, we designed and performed an assay in the presence of glutathione ethyl ester (GSH-OEt), wherein only **1** molecules internalized into cells via RME in the first 24 h period exert cytotoxic effect. The observed selectivity of **1** was remarkable with two-orders of magnitude difference in IC_{50} values between BR+ cancer cells and WI38 cells, demonstrating a salient feature of this tumor-targeted drug delivery system.

INTRODUCTION

Accounting for nearly one quarter of total deaths in the United States, cancer remains the second leading cause of death behind heart disease.[1] Traditional chemotherapy uses highly potent cytotoxic agents to interfere with the processes of cell proliferation, relying on the premise that rapidly proliferating tumor cells are more likely to be killed than normal cells. This lack of tumor-specificity continues to be a serious issue in cancer treatment, causing undesirable and dose-limiting side effects. Therefore, concentrated efforts have been directed toward the development of tumor-targeted drug delivery systems (TTDDSs), which consist of a tumor-targeting moiety (TTM) and a cytotoxic drug connected through a suitable linker system. These TTDDSs exploit the unique and intrinsic properties of cancer

*To whom correspondences should be addressed. Phone 631-632-1339; fax 631-632-7942; iwao.ojima@stonybrook.edu.

ASSOCIATED CONTENT

Supporting Information

^{1}H and ^{13}C spectra of new compounds. FACS data for the expression levels of biotin receptors in various cancer cell lines. This material is available free of charge via the Internet at http://pubs.acs.org.

The authors declare no competing financial interest.

cells to selectively deliver cytotoxic agents to the tumor. An ideal linker system must remain stable during blood circulation, but be readily cleaved to release the active agent upon internalization or accumulation in the tumor microenvironment.[2–4] With ongoing development of novel TTDDSs, it is becoming more and more important to design and develop the corresponding imaging modalities as theranostic tools to confirm the associated biological and physiological processes with enhanced sensitivity, spatial resolution, and tissue specificity.[5]

Positron emission tomography (PET) provides quantitative, real-time imaging of radioactive nuclides in living systems and allows for *in vivo* biodistribution studies for a given radiotracer. Of these PET radioisotopes, fluorine-18 ($t_{1/2}$ = 110 min) is the most commonly used PET tracer in radiodiagnostics due to its short positron linear range in tissue (2.3 mm), providing the highest resolution of PET images of all the available positron emitters.[5] The development and use of 2-[^{18}F]fluoro-2-deoxy-D-glucose ([^{18}F]FDG) marked the beginning of target-specific imaging and diagnostic techniques with fluorine-18.[6]

Vitamins are essential to the cellular growth and survival of all living cells, but cancer cells require certain vitamins even more than normal cells do to sustain their rapid cell growth and enhanced proliferation. [7, 8] Receptors for these vitamins are overexpressed on the surfaces of cancer cells to maintain extensive vitamin uptake and may serve as useful tumor-specific biomarkers for TTDDS.[8–10] The folate receptor (FR) has been well-characterized and studied extensively for its overexpression in cancer cells and solid tumors.[7] Recently, the biotin receptor (BR) was found to be overexpressed even more than the FR in a number of cancer cell lines and has emerged as a promising molecular target for TTDDS.[8, 11, 12] We have reported several fluorescent and fluorogenic probes for the BR by employing fluorescein isothiocyanate (FITC), fluorescein, and coumarin.[11, 12] Among those fluorescent probes, biotin-NHNH-FITC and biotin-PEG$_3$-FITC (**5**) were successfully used to validate highly efficient receptor-mediated endocytosis (RME) of these probes into cancer cells via the BR.[11, 12]

We have also reported the highly efficacious internalization of a biotin-linker-(taxoid-fluorescein) conjugate,[11] a (biotin)$_n$-SWNT-(taxoid-fluorescein)$_m$ conjugate (a “Trojan Horse” TTDDS),[13] and a dual-warhead conjugate of a taxoid and camptothecin[12] into BR+ cancer cells via RME. Thus, in the present study, we have selected the BR as the tumor-specific biomarker/receptor for potential theranostic applications. However, there have been few reports on ^{18}F-labeled biotin derivatives or TTDDSs designed for *in vivo* PET biodistribution studies.[14, 15] Recently, “click” chemistry using copper(I)-catalyzed azide-alkyne [3+2] cycloaddition (CuAAC) has been introduced as an orthogonal and efficient means for introduction of ^{18}F to biomolecules and radiopharmaceuticals.[16] Thus, we have incorporated this protocol into our design and synthesis of novel fluorine-probes in the present study. Although the half-life of ^{18}F is short as mentioned above, it has been shown that “^{99m}Tc-EC20”, a ^{99m}Tc-complexed to a short folate-linked peptide, reaches the FRs on tumor cells and is internalized within a few minutes in animal models.[17, 18] Thus, ^{18}F-labeled small molecule probes should serve as useful theranostic agents

RESULTS AND DISCUSSION

Rational Design of Theranostic Conjugates

We designed two theranostic conjugates, **1** and **2**, based on a highly versatile TTDD platform, consisting of a tumor-targeting module, a cytotoxic warhead with a smart linker and a triazine splitter with an acetylene-bearing tether (Figure 1). Fluorine-labeled theranostic conjugate **1** was designed to be amenable to ^{18}F-PET radiolabeling, as well as a fluorine-probe for ^{19}F NMR analysis. Fluorescein-bearing conjugate **2** was designed as a fluorescence-imaging probe for cancer-cell specific internalization of drug conjugates via receptor-mediated endocytosis (RME) using confocal fluorescence microscopy (CFM), as well as flow cytometry analysis for quantification.

Selection of tumor-targeting module

As mentioned above, we selected the biotin receptor (BR) as the molecular target for tumor-targeted or cancer-cell-specific drug delivery systems in this study. Therefore, we selected biotin as the tumor-targeting module, which is specific to cancer cells overexpressing BR.

Selection of “warhead”

We selected a highly potent next-generation taxoid, SB-T-1214 (**3**)[19, 20] as the cytotoxic warhead in this study. Our laboratory has been successfully developing next-generation taxoids, which exhibit 2–3 orders of magnitude higher potency than paclitaxel and docetaxel against multidrug-resistant and paclitaxel-resistant cancer cell lines and tumors.[20–30] A number of these next-generation taxoids have been successfully incorporated in our TTDDSs, including small-molecule drug conjugates (SMDCs),[3, 3, 11, 12, 31, 32] antibody-drug conjugates (ADCs),[33] and macromolecular DDSs.[13, 34]

“Smart” linker

We have developed highly efficient mechanism-based “smart” disulfide linkers, which can be conjugated to a cytotoxic agent on one end and a tumor-targeting module on the other. These self-immolative linkers were designed to be stable during circulation in the blood stream, but readily cleavable in the tumor microenvironment.[3, 4, 11] Once a drug conjugate is internalized into tumor cells following target-specific binding and receptor-mediated endocytosis (RME), the “smart” linker is designed to release the drug warhead through thiol-disulfide exchange with endogenous thiols, e.g., glutathione (GSH) and thioredoxin, via facile benzothiolactonization.[4, 11, 13, 35] Since the GSH level in tumor tissues (2–8 mM) is more than 1,000 times higher than that in the blood stream (1–2 μM), GSH and other endogenous thiols serve as ideal tumor-specific triggers for drug release.[11, 13, 34, 36]

Versatile TTDDS platform

Our TTDDS platform for theranostic applications is very versatile, consisting of biotin as the tumor-targeting module, next-generation taxoid **3** as the cytotoxic warhead connected to a self-immolative disulfide linker, 1,3,5-triazine splitter module, ethylene glycol oligomers to enhance aqueous solubility, and various imaging modalities. In this study, we have introduced imaging modalities such as a fluorine-labeled prosthetic for PET (conjugate **1**) in

animal models and an FITC-labeled module for fluorescence imaging (conjugate **2**) in cancer cells, both of which can readily be introduced by “click” chemistry.

Fluorescent probes

Theranostic conjugate **2** was designed as a fluorescent probe to examine a potential effect of molecular size on RME and ultimate efficacy of this TTDDS platform against cancer cell lines. To this end, we also designed a smaller drug conjugate **4**, which does not have ethylene glycol oligomers and a triazine splitter module for comparison based on cytotoxicity. [*Note*: We have reported a similar drug conjugate previously,[11] but conjugate **4** is more appropriate for comparison with conjugate **1** since it has exactly the same self-immolative disulfide linker unit as conjugate **1**.] Fluorescent probe **5**[12] was designed as a small-molecule biotin probe to compare the effect of conjugate size on internalization via RME (Figure 2). Fluorescent paclitaxel **6** was also designed to examine non-specific internalization into both BR+ and BR- or normal cell lines (Figure 2).

Synthesis of Theranostic Conjugates 1 and 2 for PET and Fluorescence Imaging

For the synthesis of theranostic conjguates **1** and **2**, we employed propargylaminotriazine-based biotin-linker-taxoid construct **7** (Scheme 7), which is ready to attach an imaging module through “click” chemistry. The synthesis of construct **7** was detailed in our recent publication on novel tumor-targeting dual-warhead drug conjugates.[12] The synthesis of conjugates **1** and **2** is illustrated in Schemes 1 and 2.

Reaction of 1-azido-11-methanesulfonyloxy-3,6,9-trioxaundecane (**8**)[37] with TBAF at 85 °C gave fluorine-labeled-PEG_3-ethylazide **9** in 95% yield (Scheme 1). In a similar manner, the coupling of FITC with 1-amino-11-azido-3,6,9-trioxaundecane (**10**)[38] in the presence of DIPEA gave fluorescence-labeled-PEG_3-ethylazide **11** in 79% yield (Scheme 1). Then, construct **7**, bearing an acetylene moiety, was subjected to copper(I)-catalyzed “click” reactions with azides **9** and **11** in the presence of copper(II) sulfate and ascorbic acid at 25 °C to give the corresponding conjugates **1** and **2** in 89 and 87% yields, respectively (Scheme 2).

Biotin-linker-taxoid conjugate **4** was synthesized through coupling of taxoid-linker activated ester **12** with biotinylhydrazine in moderate yield (Scheme 3). Biotin-linker-FITC probe **5** was synthesized through coupling of biotinyl-NH-PEG_3-$(CH_2)_2$-NH_2 with FITC in the same manner as that recently reported from our laboratory.[12] The synthesis of fluorescent taxoid probe **6** is illustrated in Scheme 4. Fluorescein was modified to its isobutyl ester **13**, followed by Mitsunobu coupling with 4-hydroxybutanoic acid to give **14**. Then, the 7-hydroxyl group of 2’-TBDMS-paclitaxel was esterified with **14** to give **15**, which was desilylated with HF/pyridine to afford fluorescent paclitaxel **6** (Scheme 4).

Biological Evaluation of Theranostic Conjugates 1 and 2

Internalization of fluorescent conjugate 2 and probe 5 by confocal fluorescence microscopy (CFM) and flow cytometry—We have shown the efficient internalization of fluorescent probe **5** into various cancer cell lines via RME.[12] Thus, probe **5** serves as an excellent reference to examine the efficiency of the internalization of

theranostic conjugate **2** into BR+ cancer cells via RME and to assess a possible effect of molecular size on the efficiency. In addition, fluorescence-labeled paclitaxel **6** was employed to assess the non-specific internalization of paclitaxel into BR+ and BR- cells, including a human normal cell line. Thus, the internalization study on these three probes should give us a fair and accurate assessment of the cancer cell targeting specificity of theranostic conjugate **2**.

Internalization of probes **2, 5**, and **6** was visualized by CFM, and the fluorescence intensity was quantified using flow cytometry. Cellular uptake of two probes **2** and **5** across three BR + cancer cell lines, L1210FR (murine leukemia), MX-1 (human breast) and ID8 (murine ovary), as well as BR- cell lines, L1210 (murine leukemia) and WI38 (human lung fibroblast), is summarized in Figure 3.

As Figure 3 shows, the extent of internalization of theranostic conjugate **2** is comparable to that of probe **5**. Nevertheless, there is a consistent trend that smaller probe **5** shows appreciably higher fluorescence intensity. Thus, it appears that there is some effect of molecular size on the internalization via RME, although there is no practical issue associated. As anticipated, there was no appreciable internalization of **2** and **5** into BR- cell lines, L1210 and WI38 (Figure 3), indicating excellent BR+ specificity of these probes. In sharp contrast, fluorescence-labeled paclitaxel **6** clearly exhibited nonspecific internalization across both BR+ and BR- cell lines (see Figure S1 in Supporting Information). Consequently, the highly target-specific and efficient internalization of **2** and **5** into BR+ cancer cell lines has been confirmed.

Time-course of the internalization of conjugate 2 into L1210FR and MX-1 cells via RME—We monitored the time-course of the internalization of conjugate **2** into L1210FR and MX-1 cells in the time period from 15 min to 24 h. These results are shown in Figure 4. In both cell lines, conjugate **2** exhibited rapid cellular uptake by RME in the first 2–3 hours of incubation, which is evident from the significant increase in fluorescence intensity by flow cytometry analysis. Then, following this initial uptake, the rate of internalization slowed down, which is likely due to the consumption of cell-surface biotin receptors via RME, forming coated vesicle of the biotin receptor–conjugate **2** complex in cytosol. As Figure 4 indicates, however, the behaviors of L1210FR and MX-1 are substantially different. The RME of conjugate **2** into MX-1 cells appears to be faster than that into L1210FR cells up to 12 hour-period, but there is a clear saturation phenomenon in MX-1 cells after 6 hours, which drastically slows down the internalization rate. In contrast, in L1210FR cells, the rate of internalization appears to be steady after the moderate slowdown after initial 3 hours so that L1210FR cells show much greater internalization of conjugate **2** after 24 hours. The results may suggest that the recycling of the biotin receptors to the cell surface in L12110FR cells are much faster than that in MX-1 cells.

Biological Evaluation of Theranostic Conjugate 1—The cytotoxicities of **1** and **4** were evaluated in four sets of assays against three BR+ cancer cell lines, L1210FR, MX-1, and ID8, and two BR- cell lines, L1210 and WI38, using the standard MTT assay.[39] Results are summarized in Tables 1 and 2. Potency of paclitaxel and taxoid **3** on these cell lines were also examined for comparison purpose.

First, L1210FR, MX-1, and ID8 (BR^+) cancer cell lines were incubated with conjugates **1** and **4** for 48 h, and the corresponding IC_{50} values were determined. As Table 1 shows, the cytotoxicity (IC_{50}) of **1** was in a range of 6–21 nM (entry 3). In sharp contrast, its cytotoxicity against normal cell line WI38 (IC_{50} 709 nM), as well as BR- leukemia cell line L1210 (IC_{50} 593 nM) was one-two orders of magnitude weaker in potency. The results clearly indicate that conjugate **1** was selectively internalized into BR+ cancer cells via RME and released the cytotoxic warhead, taxoid **3**. As anticipated, paclitaxel and taxoid **3** were practically non-selective against BR^+ and BR^- cell lines, although MX-1 and ID8 cell lines appeared to be more sensitive to these two drugs (entries 1 and 2). Smaller conjugate **4** exhibited similar results to those for conjugate **1**, but with somewhat higher potency against all cell lines used (entry 4). The results for conjugates **1** and **4** also indicate that their observed potency was 3–30 times lower than the free warhead, i.e., taxoid **3**, against three BR+ cancer cell lines. This implies that not all warheads were released after the internalization of conjugates into these cancer cells, probably due to the lack of sufficient endogenous thiols such as glutathione (GSH) under *in vitro* assay conditions. Also, 48 h incubation time might be insufficient for drug release.

Therefore, we designed and performed three sets of assays to assess the extent of the RME of conjugates **1** and **4** as well as that of drug release: (i) In the Assay 1, MX-1, L1210FR and WI38 cells were incubated with conjugates **1** and **4** for 72 h, and their IC_{50} values were determined; (ii) In the Assay 2, (a) the three cell lines were incubated with conjugates **1** and **4** for 24 h, (b) the cell culture medium was removed by thorough washing of the cells with PBS, (c) cells were resuspended and glutathione ethyl ester (GSH-OEt) (6 equivalents to conjugate) was added, and (d) the cells were incubated for additional 48 h (i.e., total incubation time was 72 h); (iii) In the Assay 3, (a) the three cells were incubated with conjugates **1** and **4** for 24 h, (b) GSH-OEt (6 equivalents to conjugate) was added to the medium, and (c) the cells were incubated for additional 48 h (total incubation time was 72 h). Thus, the Assay 1 results should provide the potency of conjugates in the same manner as that for the first assay summarized in Table 1, but for longer incubation time (48 h vs. 72 h). The Assay 2 results should indicate the extent of the internalization of conjugates in the first 24 h period with sufficient drug release inside cells, i.e., only conjugate molecules internalized into cells exert cytotoxic effect through drug release. Accordingly, this assay may mimic the corresponding *in vivo* assay conditions, wherein non-internalized conjugates would be removed from the tumor, redistributed and eventually excreted. The Assay 3 results should exhibit the mass balance of conjugates inside as well as outside of cells, by releasing the cytotoxic warhead in the whole cell culture medium at 24 h period. Thus, in principle, the results (IC_{50} values) in this assay should be very close to those for the control using taxoid **3** (entry 2). Results are summarized in Table 2.

As the Assay 1 columns for MX-1 and L1210FR cell lines show, the IC_{50} values against MX-1 cell lines are ca. 3 times smaller, indicating that an additional 24 h incubation increased the cytotoxic effect of conjugates (entries 3 and 4). However, only a slight increase in the cytotoxic effect was observed for L1210FR cell line. Also, there was practically no difference in their cytotoxic effect against WI38 cell line (entries 3 and 4).

Paclitaxel and taxoid **3** showed a slight increase in potency in this 72-h assay (entries 1 and 2), as compared to that in the 48-h assay (Table 1).

As the Assay 2 columns for MX-1 and L1210FR cell lines show, there were clear increases in potency, especially against the L1210FR cell line. The results represent the level of internalization of conjugates at the 24 h period, which show that the intracellular concentration of the released warhead did not reach that of free taxoid **3** given externally. Nevertheless, the cancer cell selectivity (BR-specificity) of conjugates **1** and **4** is quite impressive, i.e., two-orders of magnitude difference between BR+ \cancer cells and BR− WI38 cells. The results also indicate that there is no practical difference in potency between conjugate **1** and smaller-conjugate **4**. Thus, the theranostic conjugate **1** (with ^{18}F) should exhibit the same level of efficacy as that for smaller-conjugate **4** in animal tumor models *in vivo*. The cytotoxicity against WI38 was unchanged within experimental error from that observed in the Assay 1, which means that essentially no internalization of conjugates into WI38 cells occurred in both cases.

The Assay 3 results against MX-1 and L1210FR cell lines exhibited the same level of potency as that for free taxoid **3**, as anticipated. The results clearly indicate that some of each conjugate was not internalized into cancer cells. The non-internalized conjugates released free taxoid **3** in the cell culture medium upon addition of GSH-OEt, and the released taxoid **3** diffused into the cancer cell to exert its cytotoxic effect. The results proved that the mass balance in these assays are excellent and thus these assay results are valid. Interestingly, there was a 2~3-fold difference in the potency of conjugates against WI38, for some reason, which needs further investigation.

As mentioned above, it is very likely that non-internalized conjugates would be removed from tumor tissues and eventually excreted. Thus, the putative systemic toxicity of conjugates should be represented by the results in Assays 1 and 2, i.e., conjugates are essentially benign against normal cells (BR−) at the drug concentration to be used for chemotherapy.

CONCLUSION

We have designed and synthesized novel tumor-targeting theranostic conjugates **1** and **2**, which consist of biotin as the tumor-targeting module, taxoid **3** as the cytotoxic agent, a self-immolative disulfide linker for drug release, 1,3,5-triazine as the splitter module, ethylene glycol oligomers to increase aqueous solubility, and either a fluorine-labeled prosthetic in **1** for potential ^{18}F-PET imaging *in vivo* or an FITC tether in **2** for internalization and drug-release studies *in vitro*. The multi-functionalized 1,3,5-triazine-based TTDDS platform is highly versatile and applicable to a variety of imaging modalities, such as those for PET, SPECT or MRI. Rapid late-stage introduction of a fluorine prosthetic by “click” chemistry is readily applicable to multistep synthesis of ^{18}F-labeled tumor-targeting drug conjugates.

We confirmed efficient internalization of conjugate **2** in BR$^+$ cancer cells via RME based on flow cytometry and CFM analyses. As anticipated, this TTDDS exhibited very high specificity to BR+ cancer cells. Based on the comparison with a small-molecule biotin probe

5 (MW: 808), it was concluded that conjugate **2** (MW: 2,334) was internalized at a very similar level to that of smaller conjugate **5**, and thus the size of conjugate **2** imposes little effect on the efficiency of RME.

The monitoring of the time-course of the internalization of conjugate **2** into two BR+ cancer cells, L1210FR and MX-1, revealed a substantial difference in the rate of receptor-recycling to the cell surface between these two cell lines, after rapid internalization by RME in the first several hours: The recycling of the biotin receptors to the cell surface is much faster in L1210FR than in MX-1, although the rate of the initial internalization via RME appears to be faster in MX-1.

The potency and selectivity of conjugates **1** and **4** were evaluated against MX-1, L1210FR and ID8 cancer cells (BR+), as well as L1210 and WI38 cells (BR−) in the absence and presence of GSH-OEt. In the absence of GSH-OEt addition, it was found that there was 30–120 times higher selectivity (BR specificity) in three BR+ cancer cell lines for 48 h and 72 h incubation times. However, the potencies of conjugates **1** and **4** were 2–30 times lower than the free taxoid **3** in the same assay, which indicated insufficient drug release by the endogenous GSH in these cells under the *in vitro* cell culture conditions.

Accordingly, in the next assay, we examined the extent of the internalization of conjugates **1** and **4** into MX-1 (BR+), L1210FR (BR+) and WI38 (BR−) cells in the first 24 h period with sufficient drug release inside cells by addition of GSH-OEt, i.e., only conjugate molecules internalized into cells exert cytotoxic effect through drug release with additional 48 h incubation (total 72 h). Accordingly, this assay may mimic the corresponding *in vivo* assay conditions, wherein non-internalized conjugates would be removed from tumor, redistributed and eventually excreted. In this assay, it was found that the intracellular concentration of the released warhead did not reach that of free taxoid **3** given externally, while the cancer cell selectivity (BR-specificity) of conjugates **1** and **4** was remarkable with two-orders of magnitude difference between BR+ cancer cells (IC_{50} 3.85–6.60 nM) and BR- WI38 cells (IC_{50} 590–615 nM). No practical difference in potency between conjugate **1** and conjugate **4** was observed. The cytotoxicity against WI38 was unchanged within error from that observed in the first assay, confirming that essentially there was little internalization of conjugates **1** and **4** into WI38 cells in both cases.

In the third assay, which was a control experiment, GSH-OEt was added to the cell culture medium after 24 h incubation without PBS washing, followed by additional 48 h incubation. Thus, this assay against MX-1 and L1210FR cell lines should reveal the mass balance of conjugates inside as well as outside of cells. In fact, conjugates **1** and **4** showed exactly the same level of potency (IC_{50} 2.40–2.92 nM) as that for free taxoid **3** (IC_{50} 2.32–2.66 nM), as anticipated. This means that that a certain amount of conjugates, which were not internalized into cancer cells in the 24 h incubation period, existed in the cell culture medium. The results demonstrated an excellent mass balance, confirming the validity of these three assays.

Since non-internalized conjugates would be removed from tumor tissues and eventually excreted *in vivo*, conjugates **1** and **4** are essentially benign against normal cells (BR−) at the

drug concentration to be used for chemotherapy. Further studies, including the radiosynthesis of [^{18}F]-**1** and the subsequent *in vivo* biodistribution study, are actively underway in our laboratory.

EXPERIMENTAL SECTION

Caution

Taxoids have been identified as potent cytotoxic agents. Thus, these drugs and all structurally related compounds and derivatives must be considered as mutagens and reproductive hazards for both males and females. Appropriate precautions, such as the use of gloves, goggles, lab coat, labware, and fume hood, must be taken while handling the compounds at all times.

General Methods

^{1}H, ^{13}C and ^{19}F NMR spectra were measured on a Bruker 300, 400, or 500 MHz spectrometer. Melting points were measured on a Thomas–Hoover capillary melting point apparatus and are uncorrected. TLC was performed on Sorbent Technologies aluminum-backed Silica G TLC plates (Sorbent Technologies, 200 μm, 20 cm × 20 cm), and column chromatography was carried out on silica gel 60 (Merck, 230–400 mesh ASTM). Purity was determined with a Shimadzu L-2010A HPLC HT series HPLC assembly, using a Kinetex PFP column (4.6 mm × 100 mm, 2.6 μm) with acetonitrile-water system. Two analytical HPLC conditions were used and noted as a part of the characterization data for literature unknown compounds, i.e., HPLC (A): flow rate 0.4 mL/min with a gradient of 15→95% acetonitrile for the 0–12 min period, then 95 % acetonitrile for the 12–15 min period; HPLC (B): flow rate 0.4 mL/min, 95% acetonitrile flushing for the 0–15 min period. All new compounds possessed >95% purity. High resolution mass spectrometry analysis was carried out on an Agilent LC-UV-TOF mass spectrometer at the Institute of Chemical Biology and Drug Discovery, Stony Brook, NY or at the Mass Spectrometry Laboratory, University of Illinois at Urbana- Champaign, Urbana, IL.

Materials

The chemicals were purchased from Sigma-Aldrich, Fisher Scientific, and VWR International and used as received or purified before use by standard methods. Tetrahydrofuran was freshly distilled from sodium and benzophenone. Dichloromethane was also distilled immediately prior to use under nitrogen from calcium hydride. 10-Deacetylbaccatin III was a gift from Indena, SpA, Italy. Biotin-NH-PEG$_3$-(CH$_2$)$_2$-NH-FITC (**5**),[12] 4-(11-biotinylamino-3,6,9-trioxaundecyl)amino-2-propargylamino-6-[2-(SB-T-1214-SS-Linker)amidoethyl]amino-1,3,5-triazine (**7**),[12] 1-azido-11-methanesulfonyloxy-3,6,9-trioxaundecane (**8**),[37] 1-amino-11-azido-3,6,9-trioxaundecane (**10**),[38] *tert*-butyl-4-hydroxybutanoate,[11] 2'-(*tert*-butyldimethylsilyl)paclitaxel,[11] (SB-T-1214)-(SS-linker)-OSu (**12**),[12] and biotinylhydrazine,[11] were prepared by literature methods. 3-(4,5-Dimethylthiazol-2-yl)-2,5-diphenyltetrazolium bromide (MTT) was obtained from Sigma Chemical Co. Biological materials including RPMI-1640 and DMEM cell culture media, fetal bovine serum, NuSerum, PenStrep, and TrypLE were obtained from Gibco and VWR International, and used as received for cell-based assays.

1-Azido-11-fluoro-3,6,9-trioxaundecane (9)

To a solution of 1-azido-11-methanesulfonyloxy-3,6,9-trioxaundecane (**8**) (0.170 g, 0.572 mmol) in *tert*-amyl alcohol (6 mL) was added 1 M tetrabutylammonium fluoride in THF (1.7 mL, 1.7 mmol), and the mixture was stirred for 2 h at 85 °C. The reaction mixture was cooled to 25 °C and diluted with H_2O (10 mL). Then, the reaction mixture was extracted with ethyl acetate (20 mL × 3), and the combined organic layers were washed with brine (10 mL × 3), dried over $MgSO_4$, and concentrated *in vacuo* to afford a yellow liquid. Purification of the crude product by column chromatography on silica gel with 2% CH_3OH in CH_2Cl_2 as eluent gave **9** (0.120 g, 95%) as a colorless liquid: ^{1}H NMR (300 MHz, $CDCl_3$) δ 3.39 (t, *J* = 5.1 Hz, 2H), 3.67 (m, 10H), 3.75 (m, 2H), 4.57 (m, 2H); ^{13}C NMR (125 MHz, $CDCl_3$) δ 50.67, 70.01, 70.30, 70.45, 70.67, 70.79, 82.46, 83.81; ^{19}F NMR (470 MHz, $CDCl_3$) δ −45.56 (m, 1F). ^{1}H, ^{13}C, and ^{19}F NMR spectra were consistent with the reported data.[40]

Fluorine-labeled Theranostic Conjugate 1

To a solution of propargylaminotriazine construct **7**[12] (27.8 mg, 0.0174 mmol) and ascorbic acid (3.4 mg, 0.0191 mmol) in THF (0.5 mL) was added **9** (4.2 mg, 0.0191 mmol) first, followed by an aqueous solution of $CuSO_4{\cdot}5H_2O$ (5 mg, 0.0191 mmol) in H_2O (0.1 mL). The mixture was allowed to react at room temperature for 25 min, and the reaction mixture was diluted with H_2O (10 mL) and extracted with CH_2Cl_2 (10 mL × 3). The combined organic layers were dried over $MgSO_4$ and concentrated *in vacuo* to afford a milky white solid, which was triturated with hexanes (20 mL × 4) and ethyl acetate (20 mL × 4) to afford **1** (27 mg, 87%) as a white solid: mp 100–101 °C; ^{1}H NMR (500 MHz, CD_3OD) δ 0.90–1.02 (m, 7H), 1.08 (m, 1H), 1.16 (s, 3H), 1.17 (s, 3H), 1.24 (d, *J* = 6.8 Hz, 3H), 1.28 (m, 5H), 1.39 (m, 1H), 1.40 (s, 9H), 1.61 (m, 4H), 1.64 (s, 3H), 1.73 (s, 3H), 1.75 (s, 3H), 1.78 (m, 2H), 1.86 (m, 1H), 1.91 (s, 3H), 2.18 (t, *J* = 7.5 Hz, 2H), 2.22 (m, 3H), 2.38 (s, 3H), 2.54 (m, 2H), 2.68 (d, *J* = 12.8 Hz, 1H), 2.84 (m, 1H), 2.90 (dd, *J* = 5.0, 12.8 Hz, 1H), 3.16 (m, 1H), 3.34 (m, 3H), 3.41 (bs, 2H), 3.48 (m, 2H), 3.52 (t, *J* = 5.4 Hz, 2H), 3.61 (m, 4H), 3.65 (m, 20H), 3.71 (m, 2H), 3.85 (m, 3H), 4.00 (d, *J* = 16.8 Hz, 1H), 4.09 (d, *J* = 16.8 Hz, 1H), 4.20 (d, *J* = 8.4 Hz, 1H), 4.24 (d, J = 8.4 Hz, 1H), 4.27 (dd, *J* = 4.4 Hz, 8.0 Hz, 1H), 4.31 (m, 1H), 4.46 (m, 1H), 4.49 (m, 2H), 4.52 (m, 2H), 4.92 (bs, 2H), 5.00 (d, *J* = 8.4 Hz, 1H), 5.27 (bs, 1H), 5.67 (d, *J* = 7.2 Hz, 1H), 6.31 (bt, *J* = 8.5 Hz, 1H), 6.45 (s, 1H), 7.24 (m, 1H), 7.30 (m, 2H), 7.50 (t, *J* = 7.7 Hz, 2H), 7.63 (t, *J* = 7.5 Hz, 1H), 7.77 (m, 1H), 7.91 (bs, 1H), 8.12 (d, *J* = 7.5 Hz, 2H); ^{13}C NMR (125 MHz, CD_3OD) δ 7.79, 7.83, 9.05, 12.41, 13.04, 13.68, 14.04, 17.27, 19.59, 19.65, 20.97, 21.89, 22.30, 24.71, 25.47, 25.60, 27.41, 28.09, 28.37, 31.29, 31.35, 32.99, 33.08, 33.35, 36.15, 38.10, 38.99, 39.48, 39.77, 40.02, 43.21, 45.96, 46.06, 46.68, 50.09, 50.38, 55.69, 57.90, 60.20, 61.96, 65.52, 68.99, 69.19, 69.65, 69.74, 69.84, 69.90, 70.05, 70.13, 70.20, 70.23, 70.27, 70.93, 71.64, 74.94, 75.18, 75.33, 76.07, 79.31, 80.95, 82.10, 83.43, 84, 49, 119.83, 123.74, 127.58, 128.06, 128.30, 129.76, 130.02, 131.07, 132.79, 133.19, 133.45, 137.32, 141.18, 156.11, 164.68, 166.24, 168.94, 170.08, 170.97, 173.71, 174.01, 174.74, 203.78; ^{19}F NMR (282 MHz, CD_3OD) δ −46.92 (m, 1F); HRMS (TOF) for $C_{92}H_{132}N_{14}O_{25}FS_3^+$ calcd: 1947.8629. Found: 1947.8647 (Δ = 0.9 ppm). HPLC (A): t = 6.3 min, purity > 98%.

FITC-NH-PEG$_3$-(CH$_2$)$_2$-N$_3$ (11)

To a solution of fluorescein isothiocyanate (FITC) (0.200 g, 0.514 mmol) and amine **10** (0.131 g, 0.616 mmol) in DMSO (1 mL) was added triethylamine (75 μL, 0.514 mmol), and the mixture was stirred for 2 h at room temperature in the dark. The reaction mixture was concentrated *in vacuo* to afford a red oil. Purification of the crude product by column chromatography on silica gel with 7% CH_3OH in CH_2Cl_2 as eluent gave **11** (0.241 g, 79%) as an orange solid: ^{1}H NMR (500 MHz, DMSO-d_6) δ 3.42 (t, *J* = 5.0 Hz, 2H), 3.62 (m, 14H), 3.73 (bs, 2H), 6.57 (dd, *J* = 2.3, 8.7 Hz, 2H), 6.62 (d, *J* = 8.7 Hz, 2H), 6.71 (d, *J* = 2.3 Hz, 2H), 7.22 (d, *J* = 8.3 Hz, 1H), 7.78 (d, *J* = 7.8 Hz, 1H), 8.13 (bs, 1H), 8.31 (s, 1H); ^{13}C NMR (125 MHz, DMSO-d_6) δ 44.19, 50.46, 68.90, 69.72, 70.15, 70.28, 79.65, 102.70, 110.18, 113.04, 116.79, 124.54, 127.30, 129.50, 129.86, 141.79, 147.61, 151.34, 159.94, 168.98, 180.99; HRMS (TOF) for $C_{29}H_{30}N_5O_8S^+$ calcd: 608.1810. Found: 608.1822 (Δ = 2.0 ppm).

Fluorescent Theranostic Conjugate 2

To a solution of **7** (29.0 mg, 0.0167 mmol) and ascorbic acid (3.3 mg, 0.0185 mmol) in THF (0.5 mL) was added azide **11** (10.2 mg, 0.0167 mmol) first, followed by an aqueous solution of $CuSO_4{\cdot}5H_2O$ (4.6 mg, 0.0185 mmol) in H_2O (0.1 mL). The mixture was allowed to react at room temperature for 24 h in the dark. The reaction mixture was diluted with H_2O (10 mL) and extracted with CH_2Cl_2 (10 mL × 3). The combined organic layers were dried over $MgSO_4$ and concentrated *in vacuo* to afford a yellow solid, which was re-dissolved in CH_2Cl_2 and CH_3OH (9:1) and lyophilized afford **2** (0.0331 g, 85%) as a yellow solid: ^{1}H NMR (500 MHz, DMSO-d_6) δ 0.92 (m, 2H), 1.00 (m, 2H), 1.10 (s, 3H), 1.22 (d, *J* = 6.8 Hz, 3H), 1.27 (s, 3H), 1.32 (m, 2H), 1.42 (s, 9H), 1.52 (m, 4H), 1.55 (s, 3H), 1.63 (s, 3H), 1.69 (m, 2H), 1.74 (s, 3H), 1.84 (s, 3H), 1.86 (m, 1H), 2.09 (t, *J* = 7.5 Hz, 2H), 2.20 (t, *J* = 7.0 Hz, 1H), 2.25 (m, 1H), 2.36 (s, 3H), 2.60 (d, *J* = 12.5, 1H), 2.86 (dd, *J* = 5.0, 12.5, 1H), 2.95 (m, 1H), 3.12 (m, 1H), 3.22 (m, 4H), 3.29 (m, 2H), 3.41 (t, *J* = 5.5 Hz, 4H), 3.53 (m, 18H), 3.62 (m, 2H), 3.71 (d, *J* = 7.2 Hz, 2H), 3.81 (m, 2H), 4.00 (s, 2H), 4.09 (m, 2H), 4.15 (m, 2H), 4.33 (m, 1H), 4.50 (m, 2H), 4.75 (m, 1H), 4.85 (d, J = 7.9 Hz, 1H), 4.96 (m, 3H), 5.20 (m, 1H), 5.52 (d, *J* = 7.2 Hz, 1H), 6.03 (m, 1H), 6.35 (s, 1H), 6.39 (s, 1H), 6.45 (s, 1H), 6.60 (dd, *J* = 2.3, 8.7 Hz, 2H), 6.64 (d, *J* = 8.7 Hz, 2H), 6.71 (d, *J* = 2.3 Hz, 2H), 7.25 (m, 2H) 7.30 (t, *J* = 7.7 Hz, 1H), 7.34 (m, 1H), 7.40 (t, *J* = 7.7 Hz, 1H), 7.57 (t, *J* = 7.7 Hz, 2H), 7.71 (t, *J* = 7.4 Hz, 1H), 7.76 (bs, 1H), 7.78 (d, *J* = 8.0 Hz, 1H), 7.85 (m, 1H), 7.90 (bs, 1H), 8.04 (d, *J* = 7.6 Hz, 2H), 8.22 (bs, 1H); ^{13}C NMR (125 MHz, DMSO-d_6) δ 8.75, 8.83, 10.24, 13.15, 14.20, 14.23, 18.36, 19.64, 20.45, 20.52, 21.90, 22.99, 25.74, 25.95, 26.81, 28.50, 28.65, 31.57, 32.42, 32.98, 33.07, 35.56, 37.03, 38.31, 38.91, 40.91, 43.49, 46.04, 46.15, 46.69, 49.75, 55.39, 55.91, 57.96, 59.66, 61.50, 69.63, 70.02, 70.11, 70.19, 70.22, 70.89, 73.74, 75.00, 75.03, 75.06, 75.10, 75.12, 75.15, 75.27, 75.78, 77.22, 78.61, 80.88, 83.48, 84.07, 88.37, 102.71, 110.13, 110.45, 113.04, 120.71, 127.89, 128.83, 129.11, 129.50, 129.99, 130.40, 131.63, 133.32, 133.81, 133.87, 133.88, 136.45, 137.33, 137.35, 139.99, 152.37, 155.41, 159.94, 163.18, 165.50, 169.25, 170.07, 170.65, 171.92, 172.60, 172.64, 203.02; HRMS (TOF) calcd for $C_{113}H_{145}N_{16}O_{30}S_4^+$ calcd: 2333.9190. Found: 2333.9130 (Δ = −2.6 ppm). HPLC (B): RT = 5.3 min, purity > 96%.

Isobutyl 2-(6-hydroxy-3-oxo-*3H*-xanthen-9-yl)benzoate (13)

To a solution of fluorescein (1.0 g, 3.0 mmol) in isopropanol (10 mL) was added concentrated H_2SO_4 (0.75 mL), and the mixture was refluxed for 16 h at 120 °C in the dark. The reaction mixture was cooled to 25 °C and extracted with ethyl acetate (20 mL × 3). The combined organic layers were washed with saturated $NaHCO_3$ (20 mL × 3) and brine (20 mL × 3), dried over $MgSO_4$, and concentrated *in vacuo* to give a red oil. Purification of the crude product by column chromatography on silica gel with 6% CH_3OH in CH_2Cl_2 as eluent gave **13** (0.924 g, 79%) as a red solid: ^{1}H NMR (500 MHz, $CDCl_3$) δ 0.66 (d, J = 6.6 Hz, 6H), 1.57 (m, 1H), 3.74 (d, *J* = 6.6 Hz, 2H), 6.79 (dd, *J* = 2.1, 9.3 Hz, 2H), 6.87 (d, *J* = 2.1 Hz, 2H), 6.98 (d, J = 9.3 Hz, 2H), 7.30 (dd, *J* = 1.0, 7.5 Hz, 1H), 7.70 (m, 2H), 8.26 (dd, *J* = 1.0, 7.5 Hz, 1H); ^{13}C NMR (125 MHz, $CDCl_3$) δ 18.89, 27.49, 71.95, 103.70, 114.83, 122.21, 129.83, 130.37, 130.59, 130.68, 131.30, 132.49, 134.09, 155.87, 157.88, 165.47, 175.63. HRMS (TOF) for $C_{24}H_{21}O_5^+$ calcd: 389.1384. Found: 389.1400 (Δ = 4.1 ppm). HPLC (A): RT = 7.0 min, purity > 99%.

4-(9-(2-Isobutoxycarbonylphenyl)-3-oxo-*3H*-xanthen-6-yloxy)butanoic acid (14)

To a solution of **13** (0.300 g, 0.77 mmol), triphenylphosphine (0.606 g, 2.31 mmol), and diisopropyl azodicarboxylate (DIAD) (0.46 mL, 2.31 mmol) in THF (7.7 mL) was added *tert*-butyl 4-hydroxybutanoate (0.124 g, 0.77 mmol) in THF (5 mL), and the mixture was reacted for 4 h at room temperature in the dark. The reaction mixture was diluted with H_2O (10 mL), and then extracted with ethyl acetate (20 mL × 3). The combined organic extracts were dried over $MgSO_4$ and concentrated *in vacuo* to afford a red oil. Purification of the crude product by column chromatography on silica gel with hexanes/ethyl acetate (1:1) as eluent gave crude product (0.343 g) as a mixture with triphenylphosphine oxide. Then, TFA (0.6 mL) was added to a solution of the crude product in CH_2Cl_2 (2.5 mL). The reaction mixture was allowed to stir for 3 h at room temperature and concentrated *in vacuo* to give a red oil. Purification of the crude product by column chromatography on silica gel with 5% CH_3OH in CH_2Cl_2 as eluent gave **14** (0.313 g, 85% over 2 steps) as a red solid: ^{1}H NMR (500 MHz, DMSO-d_6) δ 0.62 (t, *J* = 6.3 Hz,, 3H), 0.63 (t, *J* = 6.3 Hz,, 3H), 1.55 (sept, *J* = 6.3 Hz, 1H), 1.97 (quintet, *J* = 7.0 Hz, 2H), 2.37 (t, *J* = 7.0 Hz, 2H), 3.70 (dd, *J* = 6.3, 10.7 Hz, 1H), 3.77 (dd, *J* = 6.3, 10.7, 1H), 4.16 (t, *J* = 6.2 Hz, 2H), 6.22 (d, *J* = 1.4 Hz, 1H), 6.40 (dd, *J* = 1.4, 9.7 Hz, 1H), 6.81–6.90 (m, 3H), 7.22 (d, *J* = 1.7 Hz, 1H), 7.49 (d, *J* = 7.3 Hz, 1H), 7.80 (t, *J* = 7.3 Hz, 1H), 7.87 (t, *J* = 7.3 Hz, 1H), 8.21 (d, *J* = 7.3 Hz, 1H); ^{13}C NMR (125 MHz, DMSO-d_6) δ 18.98, 19.02, 24.46, 27.51, 30.61, 68.37, 71.62, 101.44, 105.03, 114.41, 114.77, 117.21, 129.45, 129.90, 130.46, 130.52, 130.86, 131.17, 131.32, 133.55, 133.82, 150.39, 154.12, 158.87, 163.67, 165.68, 174.47, 184.30. HRMS (TOF) for $C_{28}H_{27}O_7^+$ calcd: 475.1751. Found: 475.1751 (Δ = 0 ppm). HPLC (B): RT = 6.2 min, purity > 97%.

2'-TBDMS-7-[4-[9-(2-isobutoxycarbonylphenyl)-3-oxo-*3H*-xanthen-6-yloxy]butanoyl]-paclitaxel (15)

To a solution of **14** (0.037 g, 0.078 mmol), 2'-TBDMS-paclitaxel[11] (0.038 g, 0.039 mmol), and DMAP (0.005 g, 0.039 mmol) in CH_2Cl_2–DMF (3:1) (20 mL) was added *N*,*N*'-diisopropylcarbodiimide (DIC) (12 μL, 0.078 mmol), and the mixture was reacted for 24 h at

room temperature in the dark. The reaction mixture was concentrated *in vacuo* to afford an orange oil. Purification of the crude product by column chromatography on silica gel with 2% CH_3OH in CH_2Cl_2 as eluent gave **15** (0.039 g, 70%) as a yellow solid: ^{1}H NMR (500 MHz, $CDCl_3$) δ −0.30 (s, 3H), −0.03 (s, 3H), 0.70 (m, 6H), 0.80 (s, 9H), 1.16 (s, 3H), 1.22 (s, 3H), 1.61 (m, 4H), 1.79 (s, 1H), 1.82 (s, 3H), 1.87 (m, 1H), 1.98 (s, 3H). 2.13 (m, 5H), 2.49 (m, 2H), 2.52 (t, J = 7.2 Hz, 1H), 2.54 (t, *J* = 7.2 Hz, 1H), 2.58 (s, 3H), 2.61 (m, 1H), 3.73 (m, 1H), 3.79 (d, *J* = 7.2 Hz, 1H), 3.99 (m, 1H), 4.12 (m, 2H), 4.21 (d, *J* = 8.4 Hz, 1H), 4.35 (d, *J* = 8.4 Hz, 1H), 4.70 (d, J = 2.1, 1H), 4.97 (d, *J* = 9.1 Hz, 1H), 5.64 (dd, *J* = 7.2, 10.6 Hz, 1H), 5.74 (d, J = 7.2 Hz, 1H), 5.75 (m, 1H), 6.26 (t, *J* = 9.5 Hz, 1H), 6.27 (s, 1H), 6.47 (bs, 1H), 6.56 (d, *J* = 9.0 Hz, 1H), 6.74 (d, *J* = 9.0 Hz, 1H), 6.89 (m, 2H), 6.96 (s, 1H), 7.09 (d, *J* = 9.0 Hz, 1H), 7.32 (m, 4H), 7.40 (m, 4H), 7.52 (m, 3H), 7.61 (t, *J* = 7.6 Hz, 1H), 7.67 (t, *J* = 7.6 Hz, 1H), 7.72 (t, *J* = 7.6 Hz, 1H), 7.75 (d, *J* = 7.1 Hz, 2H), 8.13 (d, *J* = 7.1 Hz, 2H), 8.26 (d, *J* = 7.6 Hz, 1H). ^{13}C NMR (125 MHz, $CDCl_3$) δ −5.79, −5.14, 10.93, 14.66, 18.14, 18.88, 20.75, 21.43, 23.03, 23.52, 23.77, 25.55, 26.38, 27.53, 30.36, 33.46, 35.62, 42.23, 43.38, 46.86, 55.07, 55.70, 67.92, 71.33, 71.80, 71.89, 74.49, 75.10, 75.24, 76.50, 78.66, 80.96, 83.95, 101.83, 105.74, 115.23, 117.92, 126.41, 127.03, 128.01, 128.80, 128.94, 129.07, 129.66, 130.24, 130.54, 130.85, 131.31, 131.85, 132.54, 132.65, 133.79, 134.12, 134.23, 138.28, 140.97, 156.85, 159.01, 167.00, 169.06, 169.98, 171.48, 172.06, 202.09. Contains trace DMF. HRMS for $C_{81}H_{90}NO_{20}Si^+$ calcd: 1424.5820. Found: 1424.5829 (Δ = 0.6 ppm).

7-(4-Fluoresceinyl)butanoylpaclitaxel (6)

To a solution of **15** (0.025 g, 0.017 mmol) in a 1:1 mixture of CH_3CN–pyridine (2 mL) and cooled to 0 °C was added 70% HF/pyridine (0.25 mL), and the mixture was stirred for 48 h at room temperature in the dark. The reaction was quenched with H_2O (10 mL) and extracted with ethyl acetate (10 mL × 3). The combined organic layers were washed with saturated $CuSO_4$ (20 mL × 3) and brine (20 mL × 3), dried over $MgSO_4$, and concentrated *in vacuo* to afford an orange oil. Purification of the crude product by column chromatography on silica gel with 2% CH_3OH in CH_2Cl_2 gave **6** (0.020 g, 87%) as an orange solid: ^{1}H NMR (500 MHz, $CDCl_3$) δ 0.68 (m, 6H), 0.88 (m, 2H), 1.14 (s, 3H), 1.25 (s, 3H), 1.62 (m, 1H), 1.82 (s, 3H), 1.88 (m, 2H), 2.04 (s, 3H), 2.11 (d, *J* = 3.0 Hz, 3H), 2.33 (m, 2H), 2.35 (m, 2H), 2.41 (s, 3H), 2.57 (m, 2H), 3.78 (m, 2H), 4.20 (d, *J* = 8.4 Hz, 1H), 4.26 (m, 2H), 4.35 (d, *J* = 8.4 Hz, 1H), 4.87 (d, *J* = 2.1 Hz, 1H), 4.97 (d, *J* = 9.3 Hz, 1H), 5.69 (d, *J* = 6.9 Hz, 1H), 5.80 (m, 2H), 6.18 (t, *J* = 8.9 Hz, 1H), 6.27 (s, 1H), 6.67 (m, 2H), 6.79 (dd, *J* = 2.3, 9.0 Hz, 1H), 6.96 (m, 2H), 7.31 (m, 2H), 7.46 (m, 2H), 7.53 (m, 3H), 7.69 (t, *J* = 7.6 Hz, 1H), 7.74 (t, *J* = 7.6 Hz, 1H), 7.84 (d, *J* = 7.1 Hz, 2H), 8.12 (d, *J* = 7.1 Hz, 2H), 8.28 (*J* = 7.6 Hz, 1H). ^{13}C NMR (125 MHz, $CDCl_3$) δ 10.87, 14.73, 18.85, 20.76, 20.91, 22.52, 22.97, 23.47, 26.39, 27.50, 29.31, 29.69, 30.92, 33.47, 35.60, 43.24, 47.19, 55.27, 56.10, 67.94, 71.57, 71.87, 73.34, 74.31, 75.46, 76.40, 78.52, 80.89, 83.93, 100.84, 105.31, 114.84, 115.65, 117.20, 127.26, 127.98, 128.52, 128.73, 128.79, 129.08, 129.84, 130.16, 130.39, 130.58, 130.75, 131.32, 132.56, 133.78, 133.96, 135.06, 137.82, 138.69, 138.74, 140.91, 148.00, 155.31, 159.38, 164.53, 166.84, 167.16, 169.01, 170.36, 172.60, 202.14. HRMS (TOF) for $C_{75}H_{76}NO_{20}^+$ calcd: 1310.4955. Found: 1310.4961 (Δ = 0.5 ppm). HPLC (B): RT = 4.9 min, purity > 99%.

Biotin-(SS-Linker)-SB-T-1214 (4)

A solution of SB-T-1214-(SS-linker)-OSu (**12**)[12] (0.069 g, 0.269 mmol) and biotinylhydrazine (0.336 g, 0.269 mmol) in a 3:1 mixture of DMSO-pyridine (2.7 mL) was cooled to 0 °C, and the mixture was reacted for 4 d at room temperature. Purification of the crude product by column chromatography on silica gel with 7% CH_3OH in CH_2Cl_2 as eluent gave **4** (0.175 g, 47%) as a white solid: ^{1}H NMR (400 MHz, CD_3OD) δ 1.02 (m, 2H), 1.10 (m, 2H), 1.20 (s, 6H), 1.30 (d, J = 6.8 Hz, 3H), 1.44 (s, 9H), 1.49 (m, 2H), 1.63 (m, 4H), 1.68 (s, 3H), 1.76 (s, 3H), 1.78 (s, 3H), 1.81 (m, 3H), 1.94 (s, 3H), 1.99 (m, 2H), 2.28 (t, *J* = 7.6 Hz, 2H), 2.35 (m, 2H), 2.41 (s, 3H), 2.48 (m, 2H), 2.71 (d, *J* = 12.7 Hz, 1H), 2.93 (dd, *J* = 5.0, 12.7 Hz, 1H), 2.98 (m, 1H), 3.22 (m, 1H), 3.87 (d, *J* = 7.2 Hz, 1H), 4.03 (d, *J* = 2.4, 16.7, 1H), 4.13 (d, *J* = 1.8, 16.7 Hz, 1H), 4.20 (d, J = 8.4 Hz, 1H), 4.24 (d, *J* = 8.4 Hz, 1H), 4.32 (m, 2H), 4.50 (dd, *J* = 4.4, 8.0 Hz, 1H), 4.59 (s, 2H), 4.94 (d, *J* = 2.4 Hz, 2H), 5.03 (d, *J* = 7.6 Hz, 1H), 5.28 (bs, 1H), 5.69 (d, *J* = 7.2 Hz, 1H), 6.16 (bt, *J* = 9.0 Hz, 1H), 6.48 (s, 1H), 7.33 (m, 3H), 7.53 (t, *J* = 8.0 Hz, 2 Hz), 7.66 (t, *J* = 7.4 Hz, 1H), 7.83 (d, *J* = 7.8 Hz, 1H), 8.15 (d, *J* = 7.2 Hz, 2H); ^{13}C NMR (125 MHz, CD_3OD) δ 7.81, 7.84, 9.06, 12.41, 13.64, 17.27, 19.46, 19.57, 20.99, 21.89, 24.73, 24.98, 25.59, 27.41, 27.96, 28.14, 30.61, 30.90, 32.98, 35.35, 36.14, 38.13, 39.03, 39.67, 43.20, 45.78, 45.90, 46.68, 49.32, 55.54, 57.88, 60.25, 61.85, 70.92, 71.58, 74.92, 75.18, 75.34, 76.06, 77.70, 79.11, 80.93, 84.49, 119.83, 127.51, 128.06, 128.30, 129.75, 130.01, 130.09, 130.12, 131.01, 133.19, 133.37, 133.53, 137.28, 137.40, 137.54, 141.24, 156.09, 164.75, 166.20, 168.91, 170.08, 170.10, 170.89, 172.67, 173.47, 173.72, 203.76; HRMS (TOF) for $C_{68}H_{90}N_5O_{19}S_3^+$ calcd: 1376.5387. Found: 1376.5397 (Δ = 0.7 ppm). HPLC (A): RT = 12.1 min, purity > 99%.

Cell Culture

All cell lines were obtained from ATCC unless otherwise noted. Cells were cultured in RPMI-1640 cell culture medium (Gibco) or DMEM (Gibco), both supplemented with 5% (v/v) heat-inactivated fetal bovine serum (FBS), 5% (v/v) NuSerum, and 1% (v/v) penicillin and streptomycin (PenStrep) at 37 °C in a humidified atmosphere with 5% CO_2. MX-1 and ID8 (obtained from University of Kansas Medical Center) cells were cultured as monolayers on 100 mm tissue culture dishes in supplemented RPMI-1640. L1210 and L1210FR (a gift from Dr. Gregory Russell-Jones, Access Pharmaceuticals Pty Ltd., Australia) were grown as a suspension in supplemented RPMI-1640, and WI-38 as a monolayer in supplemented DMEM. Cells were harvested, collected by centrifugation at 850 rpm for 5 min, and resuspended in fresh culture medium. Cell cultures were routinely divided by treatment with trypsin (TrypLE, Gibco) as needed every 2–4 days and collected by centrifugation at 850 rpm for 5 min, and resuspended in fresh cell culture medium, containing varying cell densities for subsequent biological experiments and analysis.

Incubation of Cells with Fluorescent Probes 2 and 5

Cell suspensions (3 mL) at 5×10^5 cells/mL were added to each individual well of 6-well plates, and subsequently incubated overnight in the appropriate cell culture media. The cell culture media was replaced with 5 μM solutions of **2** and **5** in cell culture media (3 mL). The cells were then incubated with the probes for various time intervals ranging from 30 min to 24 h at 37 °C. In the case of leukemia cell lines (L1210, L1210FR), each probe (1 mM) in

DMSO (15 μM) was injected directly into fresh cell suspensions to give a final concentration of 5 μM, and incubated for similar time intervals. After incubation, the cells were removed by treating with trypsin (as needed), washed twice with PBS, collected by centrifugation, and resuspended in PBS (150 μL) for CFM and flow cytometry analysis.

Flow Cytometry Analysis of the Treated Cells

Flow cytometry analysis of the cells treated with probes **2, 5** and **6** was performed with a flow cytometer, FACSCalibur, operating at a 488 nm excitation wavelength and detecting 530 nm emission wavelengths with a 30 nm bandpass filter (515–545 nm range). Cells treated as described above were resuspended in 0.5 mL of PBS. Approximately 10,000 cells were counted for each experiment using *CellQuest 3.3* software (Becton Dickinson), and the distribution of FITC fluorescence was analyzed using *WinMDI 2.8* freeware (Joseph Trotter, Scripps Research Institute).

Confocal Fluorescence Microscopy Imaging of the Treated Cells

Cells treated as described above were resuspended in 150 μL of PBS after each experiment, and dropped onto an uncoated microslide with coverslip (MatTek Corp). Confocal fluorescence microscopy (CFM) experiments were performed using a Zeiss LSM 510 META NLO two-photon laser scanning confocal microscope system, operating at a 488 nm excitation wavelength and at 527 ± 23 nm detecting emission wavelength using a 505–550 nm bandpass filter. Images for **2, 5** and **6** were captured using a C-Apochromat 63×/1.2 water (corr.) objective. Acquired data were analyzed using LSM 510 Meta software.

In Vitro Cytotoxicity Assays

The cytotoxicities (IC_{50}, nM) of paclitaxel, taxoid **3**, and conjugates **1** and **4** were evaluated against various cancer cell lines by means of the standard quantitative colorimetric MTT assay.[39] The inhibitory activity of each compound is represented by the IC_{50} value, which is defined as the concentration required for inhibiting 50% of the cell growth. Cells were harvested, collected, and resuspended in 100 μL cell culture medium at concentrations ranging from 0.5–1.5 × 10^4 cells per well in a 96-well plate. For adhesive cell types, cells were allowed to descend to the bottom of the wells overnight, and fresh medium was added to each well upon removal of the old medium.

For the MTT assay (Table 1 and the Assay 1 in Table 2) of paclitaxel, taxoid **3** and conjugates **1** and **4**, cells were resuspended in 200 μL medium with 8,000 to 10,000 cells per well of a 96-well plate and incubated at 37 °C for 24 h before drug treatment. In DMSO stock solutions, each drug or conjugate was diluted to a series of concentrations in cell culture medium to prepare test solutions. After removing the old medium, these test solutions were added to the wells in the 96-well plate to give the final concentrations ranging from 0.5 to 5,000 nM (100 μL), and the cells were subsequently cultured at 37 °C for 48 h (Table 1) or 72 h (Table 2, Assay 1). For the leukemia cell lines, L1210 and L1210FR, cells were harvested, collected, and resuspended in the test solutions ranging from 0.5 to 5,000 nM (100 μL) at 0.5 to 0.8 × 10^4 cells per well in a 96-well plate and subsequently incubated at 37 °C for 48 h (Table 1) or 72 h (Table 2, Assay 1).

In the Assay 2 (Table 2), cells were incubated with **1** or **4** at 37 °C for 24 h, and the drug medium was removed. Then, treated cells were thoroughly washed with PBS, and GSH-OEt (6 equiv. to conjugate) in cell culture medium (200 μL) was added to the wells. These cells were incubated at 37 °C for an additional 48 h, i.e., the total incubation time was 72 h.

In the Assay 3 (Table 2), cells were incubated with **1** or **4** at 37 °C for 24 h, and GSH-OEt (6 equivalents) in cell culture medium (100 μL) was directly added to the wells. These cells were incubated at 37 °C for an additional 48 h, i.e. the total incubation time was also 72 h.

For all experiments, after removing the test medium, fresh solution of MTT in PBS (40 μL of 0.5 mg MTT/mL) was added to the wells, and the cells were incubated at 37 °C for 3 h. The MTT solution was then removed, and the resulting insoluble violet formazan crystals were dissolved in 0.1 N HCl in isopropanol with 10% Triton X-100 (40 μL) to give a violet solution. The spectrophotometric absorbance measurement of each well in the 96-well plate was run at 570 nm using a Labsystems Multiskan Ascent microplate reader. The IC_{50} values and their standard errors were calculated from the viability-concentration curve using Four Parameter Logistic Model of *Sigmaplot*. The concentration of DMSO per well was ≤1% in all cases. Each experiment was run in triplicate.

Supplementary Material

Refer to Web version on PubMed Central for supplementary material.

ACKNOWLEDGMENTS

This research was supported by a grant from the National Institutes of Health (CA 103314 to I.O.). The authors thank Dr. Guo-Wei Tian at the Central Microscopy Imaging Center of Stony Brook University for his technical assistance with confocal microscopy, as well as Dr. Anne Savitt and Rebecca Rowehl for their valuable help with cell culture preparations at the Cell Culture and Hybridoma Facility at Stony Brook University. A generous gift of 10-deacetylbaccatin III from Indena, SpA is gratefully acknowledged. The authors would like to thank Dr. Joanna Fowler and Dr. Sung Won Kim at Brookhaven National Laboratory (BNL) for valuable discussions regarding PET imaging and ^{18}F-radiosynthesis.

Abbreviations

ADC	antibody-drug conjugate
BR	biotin receptor
CFM	confocal fluorescence microscopy
DIAD	diisopropyl azodicarboxylate
DIC	*N*,*N*’-diisopropylcarbodiimide
DIPEA	*N*,*N*-diisopropylethylamine
DMEM	Dulbecco’s Modified Eagle Medium
FITC	fluorescein isothiocyanate
FR	folate receptor
GSH	glutathione

MTT	3-(4,5-dimethylthiazol-2-yl)-2,5-diphenyltetrazolium bromide
RME	receptor-mediated endocytosis
RPMI-1640	Roswell Park Memorial Institute medium
SMDC	small-molecule drug conjugate
SWNT	single-walled carbon nanotube
TBDMS	*tert*-butyldimethylsilyl
TTDD	tumor-targeted drug delivery
TTDDS	tumor-targeted drug delivery system
TTM	tumor-targeting moiety

REFERENCES

1. Heron M. Deaths: leading causes for 2010. Natl. Vital Stat. Rep. 2013; 62:1–97. [PubMed: 24364902]
2. Jaracz S, Chen J, Kuznetsova LV, Ojima I. Recent advances in tumor-targeting anticancer drug conjugates. Bioorg. Med. Chem. 2005; 13:5043–5054. [PubMed: 15955702]
3. Ojima I. Guided molecular missiles for tumor-targeting chemotherapy--case studies using the second-generation taxoids as warheads. Acc. Chem. Res. 2008; 41:108–119. [PubMed: 17663526]
4. Seitz JD, Vineberg JG, Wei L, Khan JF, Lichtenthal B, Feng C-F, Ojima I. Design, synthesis, and application of fluorine-labeled taxoids as 19F NMR probes for the metabolic stability assessment of tumor-targeted drug delivery systems. J. Fluor. Chem. 2014
5. Miller PW, Long NJ, Vilar R, Gee AD. Synthesis of 11C, 18F, 15O, and 13N radiolabels for positron emission tomography. Angew. Chem. Int. Ed. Engl. 2008; 47:8998–9033. [PubMed: 18988199]
6. Fowler JS, Ido T. Initial and subsequent approach for the synthesis of ^{18}FDG. Semin. Nucl. Med. 2002; 32:6–12. [PubMed: 11839070]
7. Leamon CP, Reddy JA. Folate-targeted chemotherapy. Adv. Drug Deliv. Rev. 2004; 56:1127–1141. [PubMed: 15094211]
8. Russell-Jones G, McTavish K, McEwan J, Rice J, Nowotnik D. Vitamin-mediated targeting as a potential mechanism to increase drug uptake by tumours. J. Inorg. Biochem. 2004; 98:1625–1633. [PubMed: 15458825]
9. Leamon CP. Folate-targeted drug strategies for the treatment of cancer. Curr. Opin. Invest. Drugs. 2008; 9:1277–1286.
10. Lu Y, Low PS. Folate-mediated delivery of macromolecular anticancer therapeutic agents. Adv. Drug Deliv. Rev. 2002; 54:675–693. [PubMed: 12204598]
11. Chen S, Zhao X, Chen J, Kuznetsova L, Wong SS, Ojima I. Mechanism-based tumor-targeting drug delivery system. Validation of efficient vitamin receptor-mediated endocytosis and drug release. Bioconjugate Chem. 2010; 21:979–987.
12. Vineberg JG, Zuniga ES, Kamath A, Chen YJ, Seitz JD, Ojima I. Design, Synthesis and Biological Evaluations of Tumor-Targeting Dual-Warhead Conjugates for a Taxoid-Camptothecin Combination Chemotherapy. J. Med. Chem. 2014; 57:5777–5791. [PubMed: 24901491]
13. Chen J, Chen S, Zhao X, Kuznetsova LV, Wong SS, Ojima I. Functionalized single-walled carbon nanotubes as rationally designed vehicles for tumor-targeted drug delivery. J. Am. Chem. Soc. 2008; 130:16778–16785. [PubMed: 19554734]
14. Shoup TM, Fischman AJ, Jaywook S, Babich JW, Strauss HW, Elmaleh DR. Synthesis of fluorine-18-labeled biotin derivatives: biodistribution and infection localization. J. Nucl. Med. 1994; 35:1685–1690. [PubMed: 7931672]

15. Kudo T, Ueda M, Konishi H, Kawashima H, Kuge Y, Mukai T, Miyano A, Tanaka S, Kizaka-Kondoh S, Hiraoka M, Saji H. PET imaging of hypoxia-inducible factor-1-active tumor cells with pretargeted oxygen-dependent degradable streptavidin and a novel ^{18}F-labeled biotin derivative. Mol. Imaging Biol. 2011; 13:1003–1010. [PubMed: 20838908]
16. Marik J, Sutcliffe JL. Click for PET: rapid preparation of [^{18}F]fluoropeptides using Cu(I) catalyzed 1,3-dipolar cycloaddition. Tetrahedron Lett. 2006; 47:6681–6684.
17. Sega EI, Low PS. Tumor detection using folate receptor-targeted imaging agents. Cancer Metastasis Rev. 2008; 27:655–664. [PubMed: 18523731]
18. Leamon CP, Parker MA, Vlahov IR, Xu LC, Reddy JA, Vetzel M, Douglas N. Synthesis and biological evaluation of EC20: a new folate-derived, (99m)Tc-based radiopharmaceutical. Bioconjugate Chem. 2002; 13:1200–1210.
19. Ojima I, Chen J, Sun L, Borella C, Wang T, Miller M, Lin S, Geng X, Kuznetsova L, Qu C, Gallagher G, Zhao X, Zanardi I, Xia S, Horwitz S, Clair JS, Guerriero J, Bar-Sagi D, Veith J, Pera P, Bernacki R. Design, Synthesis, and Biological Evaluation of New-Generation Taxoids. J. Med. Chem. 2008; 51:3203–3221. [PubMed: 18465846]
20. Ojima I, Das M. Recent advances in the chemistry and biology of new generation taxoids. J. Nat. Prod. 2009; 72:554–565. [PubMed: 19239240]
21. Ojima I, Slater JC, Michaud E, Kuduk SD, Bounaud PY, Vrignaud P, Bissery MC, Veith JM, Pera P, Bernacki RJ. Syntheses and structure-activity relationships of the second-generation antitumor taxoids: exceptional activity against drug-resistant cancer cells. J. Med. Chem. 1996; 39:3889–3896. [PubMed: 8831755]
22. Ojima I, Chen J, Sun L, Borella CP, Wang T, Miller ML, Lin S, Geng X, Kuznetsova L, Qu C, Gallager D, Zhao X, Zanardi I, Xia S, Horwitz SB, Mallen-St Clair J, Guerriero JL, Bar-Sagi D, Veith JM, Pera P, Bernacki RJ. Design, synthesis, and biological evaluation of new-generation taxoids. J. Med. Chem. 2008; 51:3203–3221. [PubMed: 18465846]
23. Kuznetsova LV, Pepe A, Ungureanu IM, Pera P, Bernacki RJ, Ojima I. Syntheses and Structure-Activity Relationships of Novel 3'-Difluoromethyl and 3'-Trifluoromethyl-Taxoids. J. Fluor. Chem. 2008; 129:817–828. [PubMed: 19448839]
24. Kuznetsova L, Sun L, Chen J, Zhao X, Seitz J, Das M, Li Y, Veith JM, Pera P, Bernacki RJ, Xia S, Horwitz SB, Ojima I. Synthesis and Biological Evaluation of Novel 3'-Difluorovinyl Taxoids. J. Fluor. Chem. 2012; 143:177–188. [PubMed: 23139432]
25. Kovar J, Ehrlichova M, Smejkalova B, Zanardi I, Ojima I, Gut I. Comparison of cell death-inducing effect of novel taxane SB-T-1216 and paclitaxel in breast cancer cells. Anticancer Res. 2009; 29:2951–2960. [PubMed: 19661300]
26. Ojima I, Lin S, Slater JC, Wang T, Pera P, Bernacki RJ, Ferlini C, Scambia G. Syntheses and biological activity of C-3'-difluoromethyl-taxoids. Bioorg. Med. Chem. 2000; 8:1619–1628. [PubMed: 10976509]
27. Ojima I, Slater JC, Kuduk SD, Takeuchi CS, Gimi RH, Sun CM, Park YH, Pera P, Veith JM, Bernacki RJ. Syntheses and structure-activity relationships of taxoids derived from 14 beta-hydroxy-10-deacetylbaccatin III. J. Med. Chem. 1997; 40:267–278. [PubMed: 9022793]
28. Bissery MC, Nohynek G, Sanderink GJ, Lavelle F. Docetaxel (Taxotere): a review of preclinical and clinical experience. Part I: Preclinical experience. Anti-cancer Drugs. 1995; 6:339–355. [PubMed: 7670132]
29. Fojo AT, Ueda K, Slamon DJ, Poplack DG, Gottesman MM, Pastan I. Expression of a multidrug-resistance gene in human tumors and tissues. Proc. Natl. Acad. Sci. U.S.A. 1987; 84:265–269. [PubMed: 2432605]
30. Gottesman MM, Pastan I. Biochemistry of multidrug resistance mediated by the multidrug transporter. Annu. Rev. Biochem. 1993; 62:385–427. [PubMed: 8102521]
31. Kuznetsova L, Chen J, Sun L, Wu X, Pepe A, Veith JM, Pera P, Bernacki RJ, Ojima I. Syntheses and evaluation of novel fatty acid-second-generation taxoid conjugates as promising anticancer agents. Bioorg. Med. Chem. Lett. 2006; 16:974–977. [PubMed: 16298526]
32. Ojima I, Zuniga ES, Berger WT, Seitz JD. Tumor-targeting drug delivery of new-generation taxoids. Future Med. Chem. 2012; 4:33–50. [PubMed: 22168163]

33. Ojima I, Geng X, Wu X, Qu C, Borella CP, Xie H, Wilhelm SD, Leece BA, Bartle LM, Goldmacher VS, Chari RV. Tumor-specific novel taxoid-monoclonal antibody conjugates. J. Med. Chem. 2002; 45:5620–5623. [PubMed: 12477344]

34. Banerjee PS, Zuniga ES, Ojima I, Carrico IS. Targeted and armed oncolytic adenovirus via chemoselective modification. Bioorg. Med. Chem. Lett. 2011; 21:4985–4988. [PubMed: 21669527]

35. Ojima I. Use of fluorine in the medicinal chemistry and chemical biology of bioactive compounds--a case study on fluorinated taxane anticancer agents. ChemBioChem. 2004; 5:628–635. [PubMed: 15122634]

36. Zheng ZB, Zhu G, Tak H, Joseph E, Eiseman JL, Creighton DJ. N-(2-hydroxypropyl)methacrylamide copolymers of a glutathione (GSH)-activated glyoxalase i inhibitor and DNA alkylating agent: synthesis, reaction kinetics with GSH, and in vitro antitumor activities. Bioconjugate Chem. 2005; 16:598–607.

37. Luo Z, Ding X, Hu Y, Wu S, Xiang Y, Zeng Y, Zhang B, Yan H, Zhang H, Zhu L, Liu J, Li J, Cai K, Zhao Y. Engineering a hollow nanocontainer platform with multifunctional molecular machines for tumor-targeted therapy in vitro and in vivo. ACS Nano. 2013; 7:10271–10284. [PubMed: 24127723]

38. Schwabacher AW, Lane JW, Schiesher MW, Leigh KM, Johnson CW. Desymmetrization reactions: Efficient preparation of unsymmetrically substituted linker molecules. J. Org. Chem. 1998; 63:1727–1729.

39. Mosmann T. Rapid colorimetric assay for cellular growth and survival: application to proliferation and cytotoxicity assays. J. Immunol. Methods. 1983; 65:55–63. [PubMed: 6606682]

40. Breyholz HJ, Wagner S, Faust A, Riemann B, Holtke C, Hermann S, Schober O, Schafers M, Kopka K. Radiofluorinated pyrimidine-2,4,6-triones as molecular probes for noninvasive MMP-targeted imaging. ChemMedChem. 2010; 5:777–789. [PubMed: 20373323]

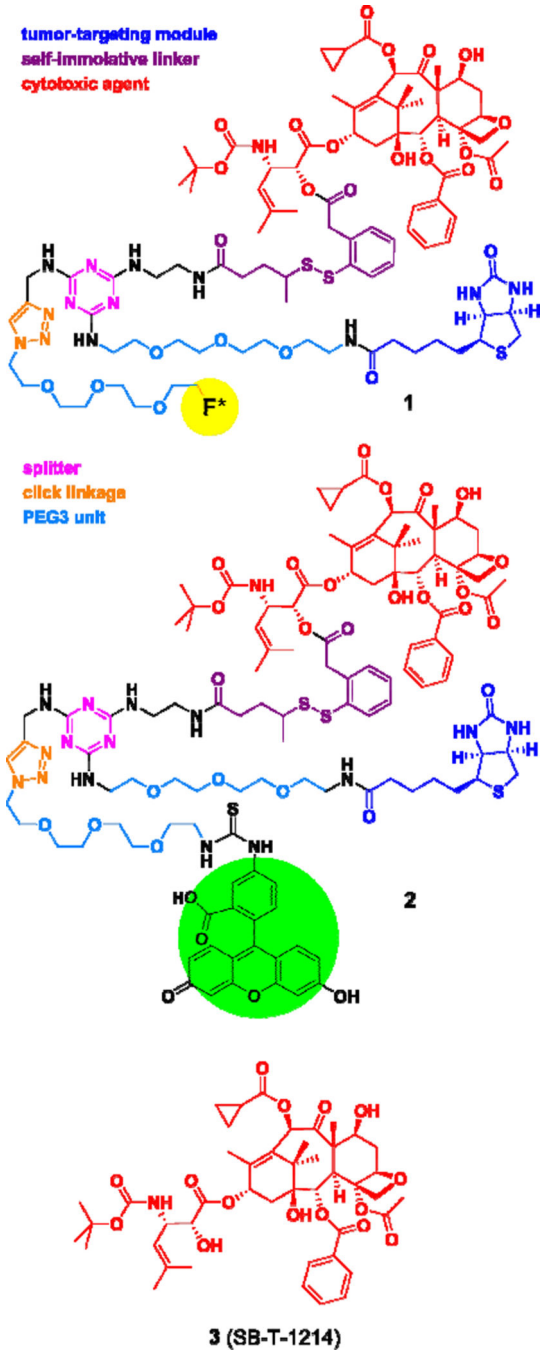

Figure 1.
Chemical structures of theranostic conjugates **1** and **2** as well as taxoid **3**

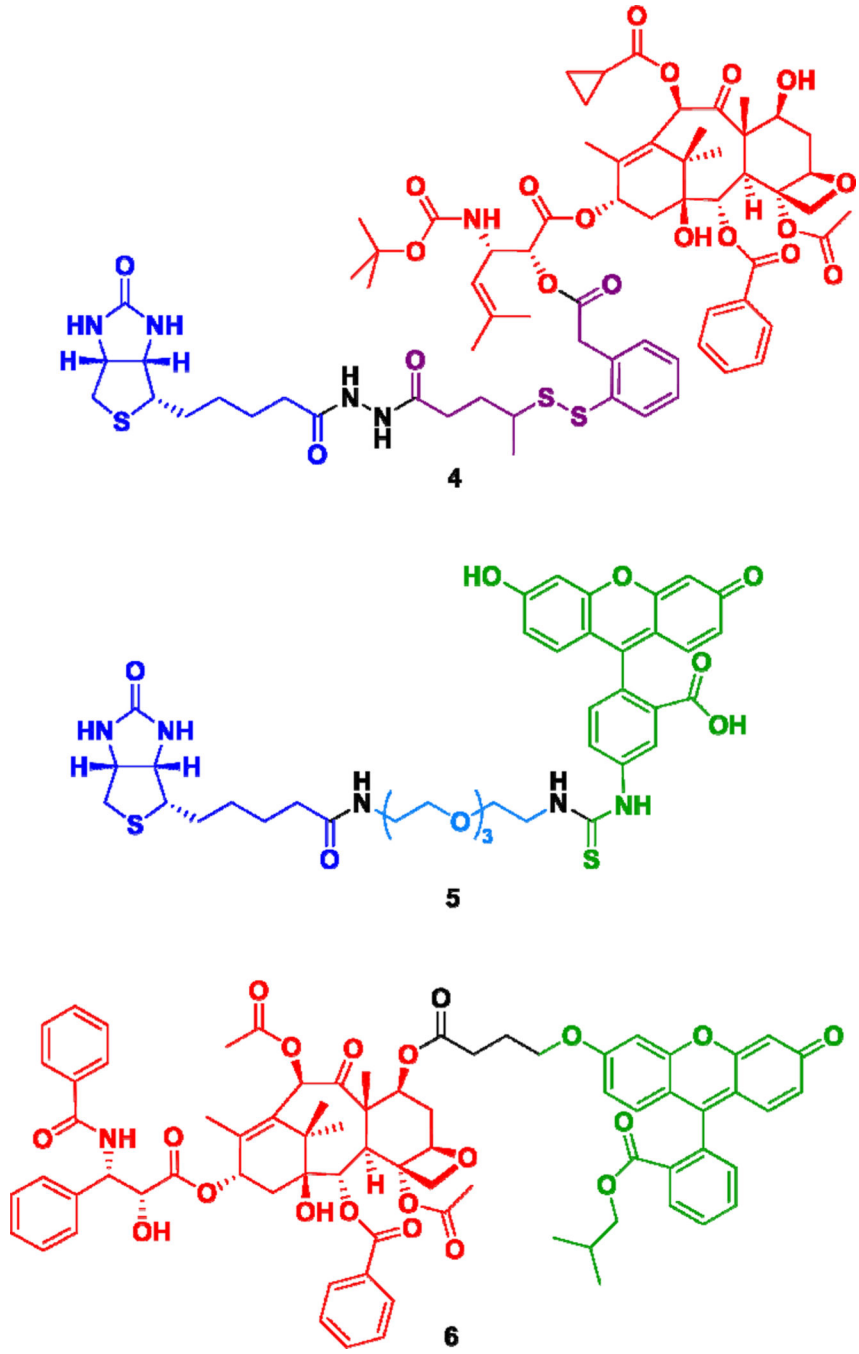

Figure 2.
Biotin-linker-taxoid conjugate (**4**) and two fluorescent probes, **5** and **6**.

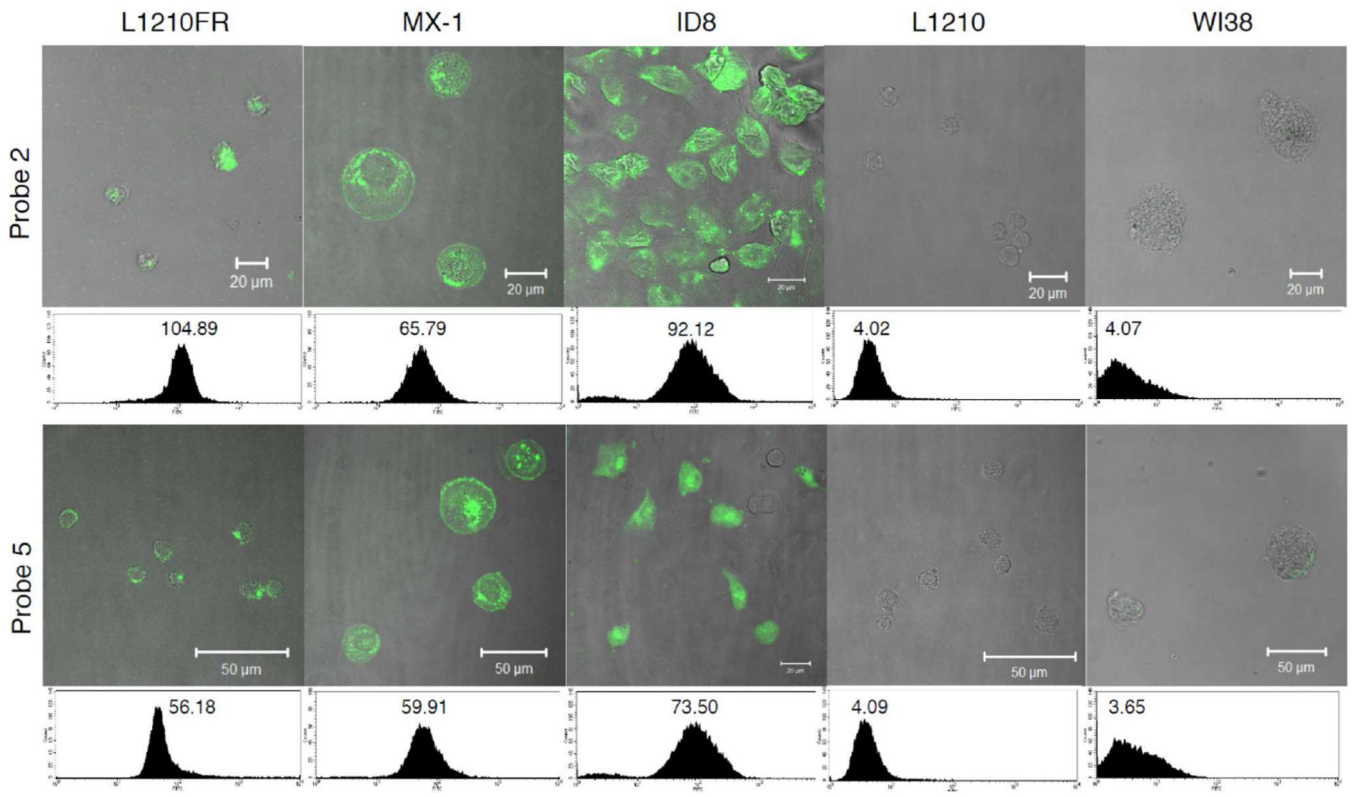

Figure 3.

CFM images and flow cytometry analysis of L1210FR (BR+), MX-1 (BR+), ID8 (BR+), L1210 (BR−), and WI38 (BR−) cell lines after incubation with conjugate **2** (5 μM) (upper row) or probe **5** (5 μM) (lower row) at 37 °C for 3

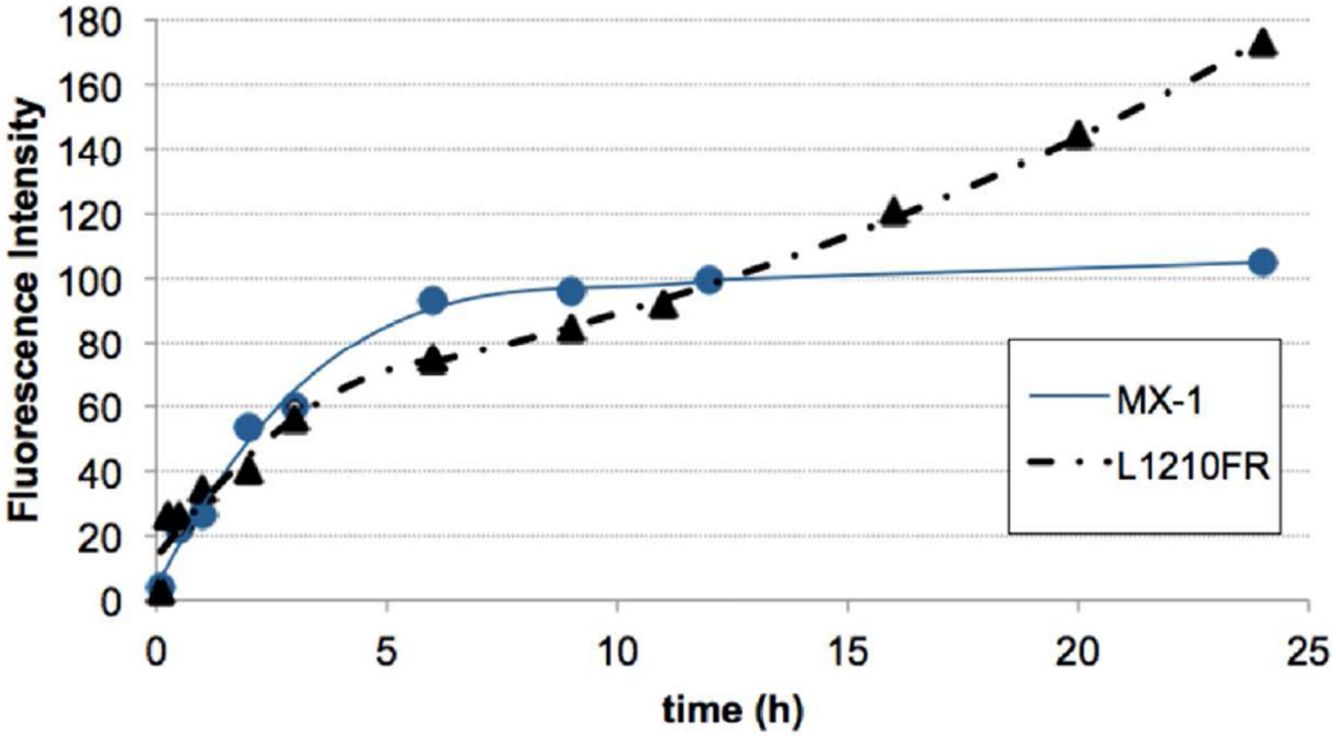

Figure 4.

Time-course of the internalization of conjugate **2** (5 μM) in L1210FR (BR+, solid triangle) and MX-1 (BR+, solid circle) cells at 37 °C by flow cytometry analysis.

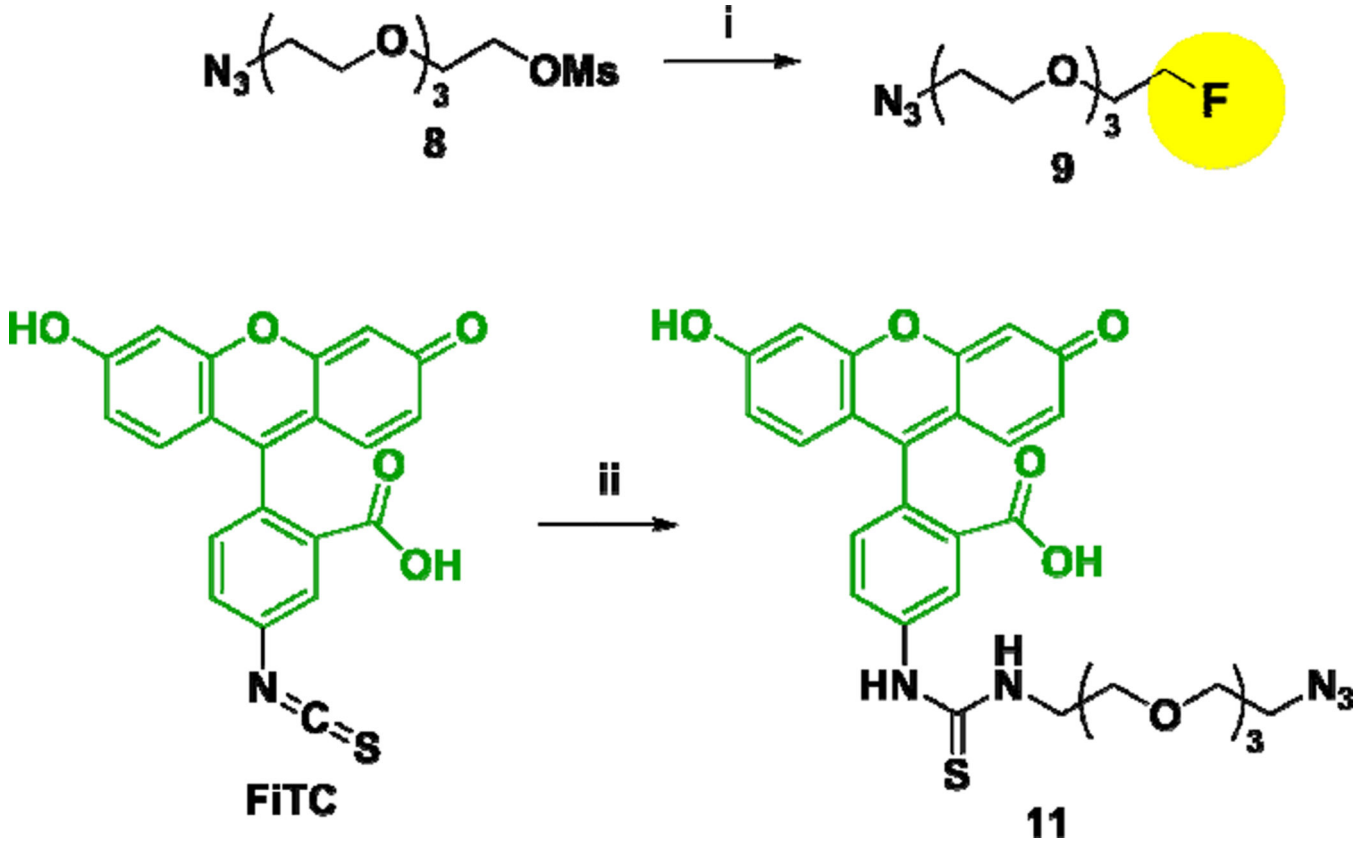

Scheme 1a.

[a]Reagents and conditions: (i) TBAF, *tert*-amyl alcohol, 85 °C, 3 h, 95%; (ii) 1-amino-11-azido-3,6,9-trioxa-undecane (**10**), Et_3N, DMSO, 25 °C, 2 h, dark, 79%.

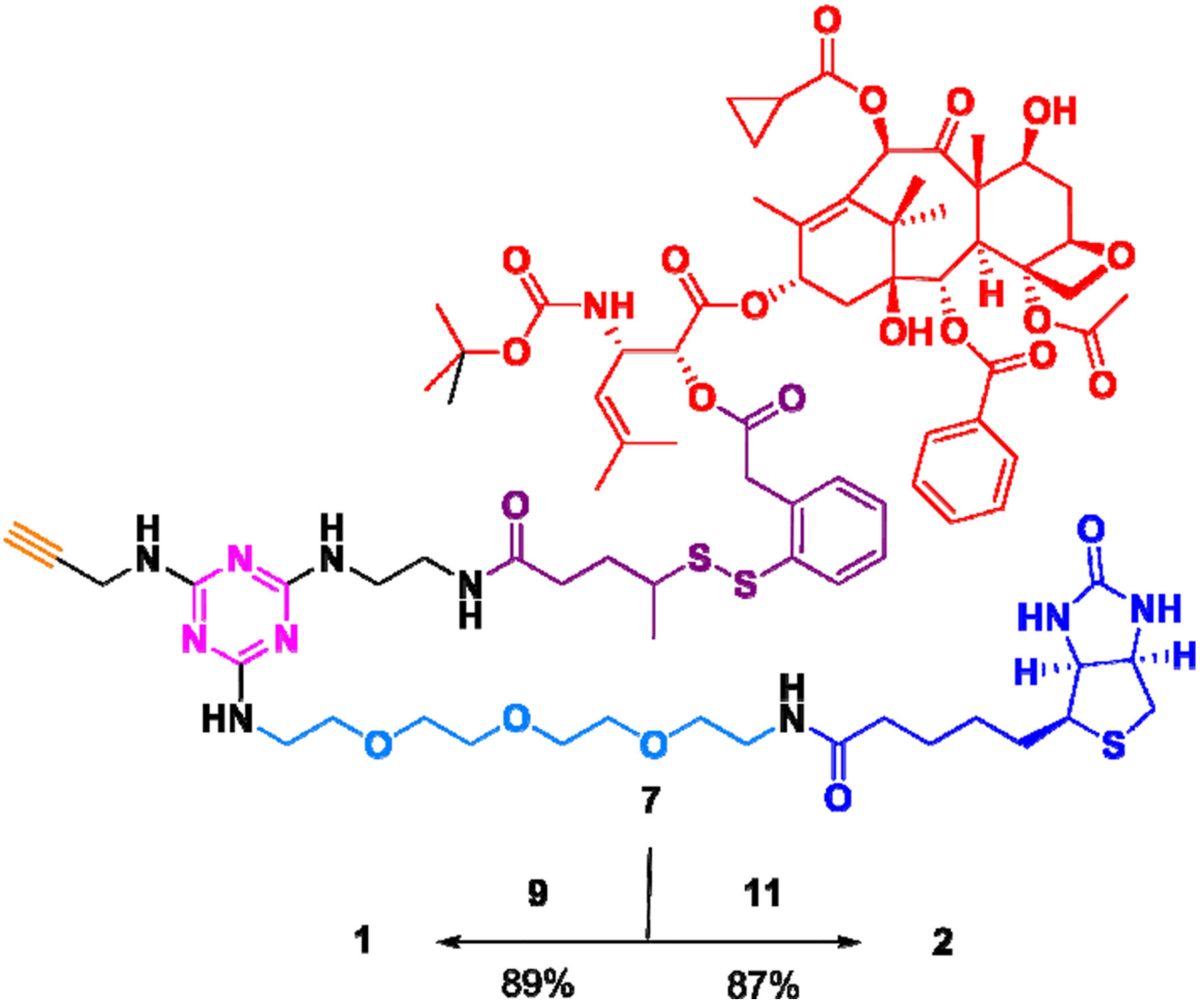

Scheme 2a.

[a]Reagents and conditions: $CuSO_4 \cdot 5H_2O$, ascorbic acid, THF/H_2O, 25 °C, 25 min.

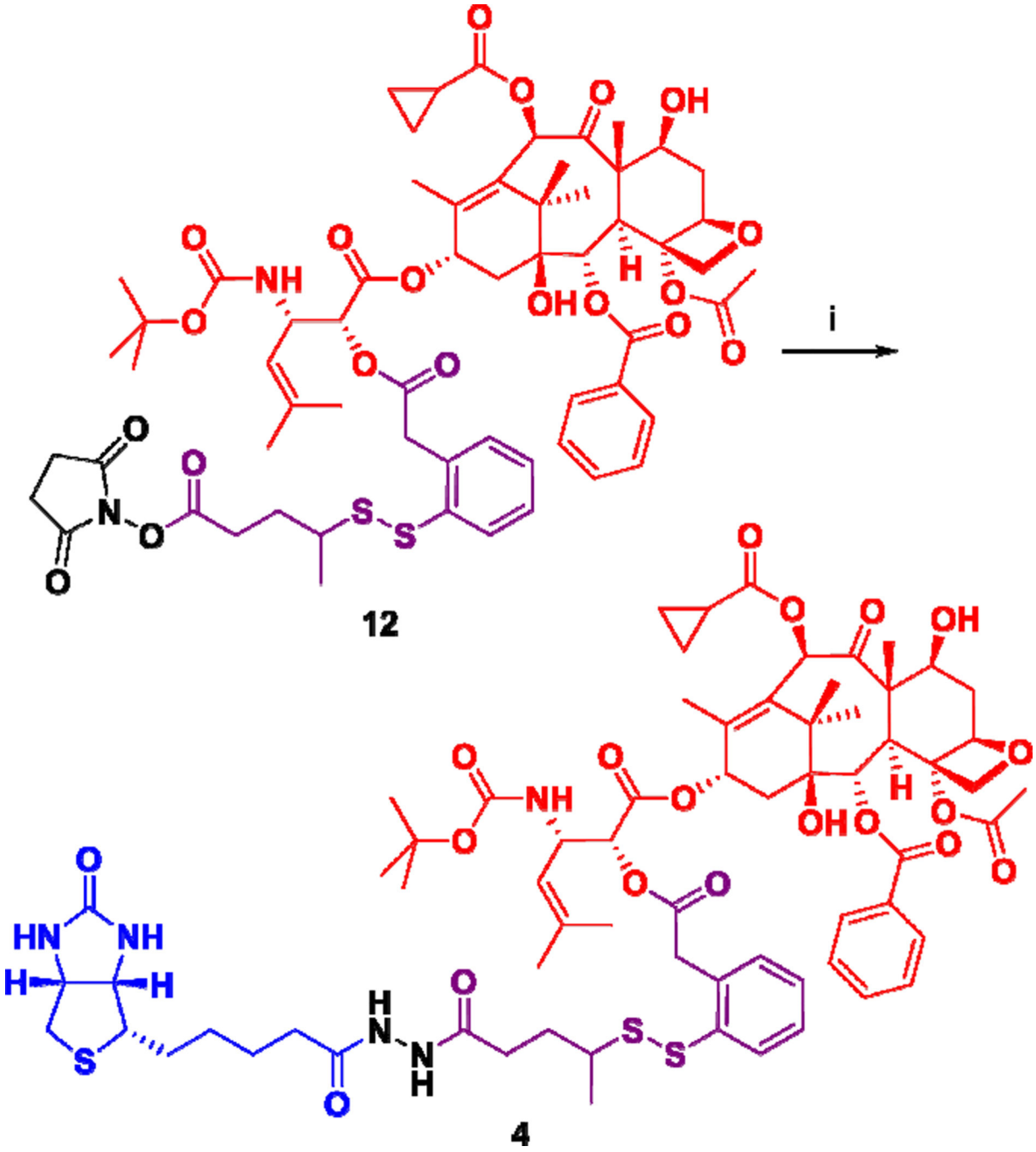

Scheme 3a.

[d]Reagents and conditions: (i) biotinylhydrazine, pyridine, DMSO, 0 °C to 25 °C, 4 d, 47%.

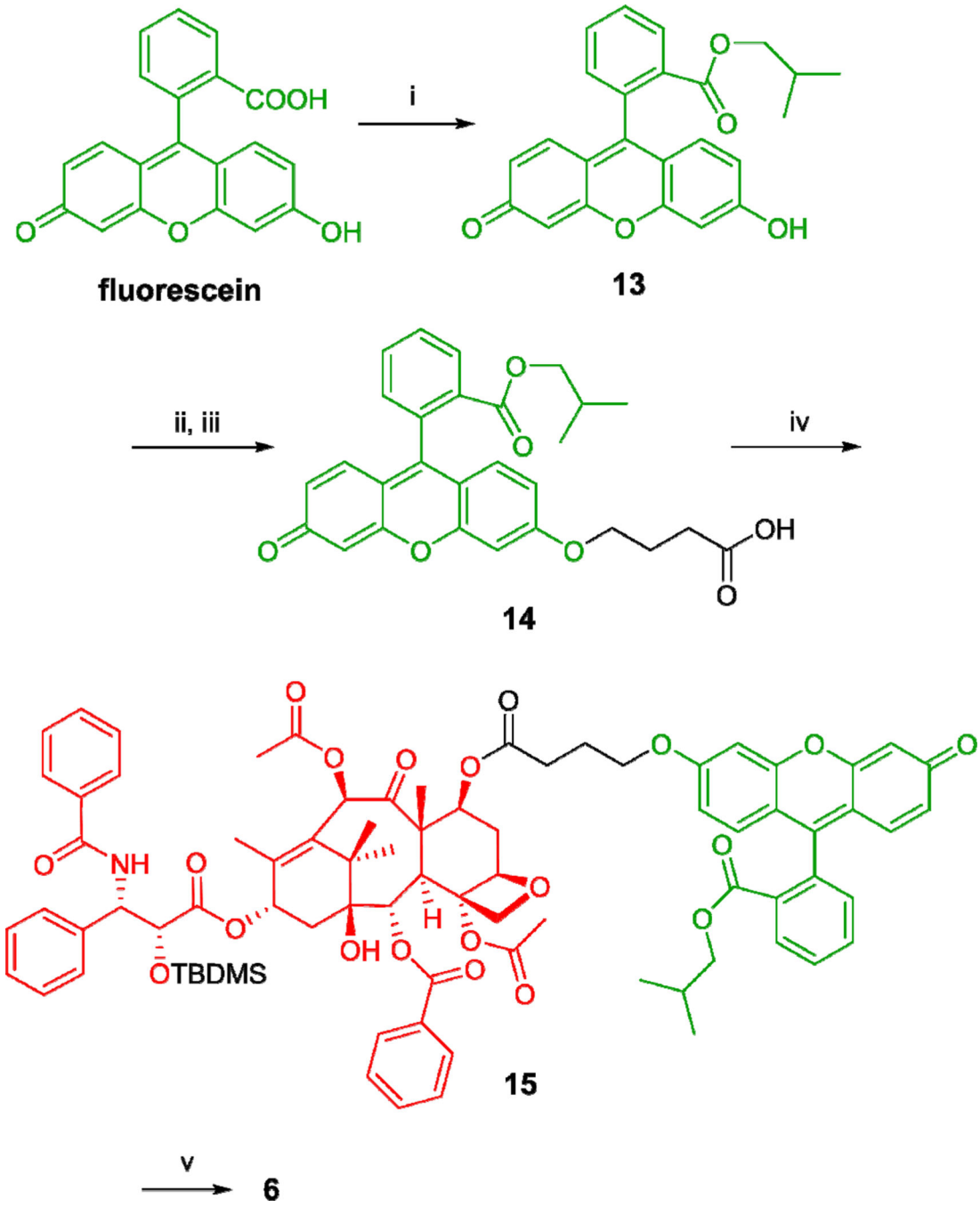

Scheme 4a.

[d]Reagents and conditions: (i) isobutanol, H_2SO_4, 120 °C, reflux, 16 h, dark, 79%; (ii) *tert*-butyl hydroxybutanoate, Ph_3P, DIAD, THF, 25 °C, 4 h, dark; (iii) TFA, CH_2Cl_2, 25 °C, 3 h, dark, 85% over 2 steps; (iv) 2'-TBDMS-paclitaxel, DIC, DMAP, CH_2Cl_2/DMF, 25 °C, 24 h, dark, 70%; (v) HF/pyridine, CH_3CN/pyridine; 0 °C to 25°C, 48 h, dark, 87%.

Table 1

Cytotoxicities (IC_{50}, nM) of Paclitaxel, Taxoid 3, Conjugates 1 and 4 against BR+ and BR− Cell Lines (Incubation at 37 °C for 48 h)

Entry	Compound	MX-1[a]	ID8[b]	L1210FR[c]	L1210[d]	WI38[e]
1[f]	paclitaxel	7.23 ± 0.68	14.36 ± 1.81	38.7 ± 17.7	77.1 ± 12.8	61.4 ± 12.7
2[f]	Taxoid **3**	4.13 ± 2.59	0.17 ± 0.14	4.18 ± 1.8	7.05 ± 1.38	5.23 ± 0.27
3[f]	**1**	21.2 ± 4.6	6.62 ± 0.86	14.7 ± 4.0	593 ± 123	709 ± 55
4[f]	**4**	15.4 ± 4.2	4.32 ± 1.58	13.4 ± 6.8	481 ± 34	670 ± 89

[a] human breast carcinoma cell line (BR+);

[b] murine ovarian carcinoma cell line (BR+);

[c] murine lymphocytic leukemia cell line (BR+);

[d] murine lymphocytic leukemia cell line (BR−);

[e] Human lung fibroblast cell line (BR−);

[f] Cells were incubated with a drug or conjugate at 37 °C for 48 h.

Table 2

Cytotoxicities (IC_{50}, nM) of Paclitaxel, Taxoid 3, Conjugate 1 and Conjugate 4 in the Absence and Presence of GSH-OEt

Entry	Compound	MX-1[a]			L1210FR[c]			WI38[e]		
		Assay 1[b]	Assay 2[d]	Assay 3[f]	Assay 1[b]	Assay 2[d]	Assay 3[f]	Assay 1[b]	Assay 2[d]	Assay 3[f]
1	paclitaxel	4.07 ± 0.80			35.6 ± 8.2			55.7 ± 9.54		
2	taxoid **3**	2.66 ± 0.16			2.32 ± 1.41			4.89 ± 2.24		
3	**1**	6.27 ± 2.06	4.79 ± 0.12	2.56 ± 0.15	10.2 ± 3.0	6.60 ± 3.96	2.79 ± 1.43	682 ± 110	615 ± 97	12.9 ± 4.3
4	**4**	4.66 ± 0.87	3.85 ± 0.14	2.40 ± 0.18	12.3 ± 2.8	5.15 ± 2.85	2.92 ± 2.34	645 ± 97	590 ± 164	11.0 ± 3.1

[a,e,e] See captions for cell lines in Table 1;

[b] Cells were incubated with a drug or conjugate at 37 °C in a 5% CO_2 atmosphere for 72 h;

[d] Cells were initially incubated with **1** or **4** at 37 °C in a 5% CO_2 atmosphere for 24 h, followed by washing of the drug media with PBS, then addition of GSH-OEt (6 equiv. to conjugate) for drug release and additional incubation for 48 h;

[f] Cells were initially incubated with **1** or **4** at 37 °C in a 5% CO_2 atmosphere for 24 h, followed by addition of GSH-OEt (6 equiv. to conjugate) for drug release and additional incubation for 48 h. Total drug or conjugate incubation was 72 h for all experiments.